Effects of rheumatoid arthritis associated transcriptional changes on osteoclast differentiation network in the synovium

Shilpa Harshan [1], **Poulami Dey** [1, 2], **Srivatsan Ragunathan** Corresp. [1]

[1] Institute of Bioinformatics and Applied Biotechnology, Bangalore, Karnataka, India

[2] Manipal Academy of Higher Education, Manipal, Karnataka, India

Corresponding Author: Srivatsan Ragunathan
Email address: srivatsan@ibab.ac.in

Background. Osteoclast differentiation in the inflamed synovium of rheumatoid arthritis affected joints leads to the formation of bone lesions. Reconstruction and analysis of protein interaction networks underlying specific disease phenotypes are essential for designing therapeutic interventions. In this study we have created a network that captures signal flow leading to osteoclast differentiation. Based on transcriptome analysis, we have indicated the potential mechanisms responsible for the phenotype in the rheumatoid arthritis affected synovium.

Method. We collected information on gene expression, pathways and protein interactions related to rheumatoid arthritis from literature and databases namely Gene Expression Omnibus, KEGG pathway and STRING. Based on these information, we created a network for the differentiation of osteoclasts. We identified the differentially regulated network genes and reported the signaling that are responsible for the process in the rheumatoid arthritis affected synovium.

Result. Our network reveals the mechanisms underlying the activation of the Neutrophil Cytosolic Factor complex in connection to osteoclastogenesis in rheumatoid arthritis. Additionally, the study reports the predominance of the canonical pathway of NF-κB activation in the diseased synovium. The network also confirms that the upregulation of T cell receptor signaling and downregulation of TGFβ signaling pathway favour osteoclastogenesis in Rheumatoid Arthritis. To the best of our knowledge, this is the first comprehensive protein-protein interaction network describing Rheumatoid Arthritis driven osteoclastogenesis in the synovium.

Discussion. This study provides information that can be used to build models of the signal flow involved in the process of osteoclast differentiation. The models can further be used to design therapies to ameliorate bone destruction in the Rheumatoid Arthritis affected joints.

Effects of Rheumatoid Arthritis associated transcriptional changes on osteoclast differentiation network in the synovium

Shilpa Harshan[1, +], Poulami Dey[1, 2, +], Srivatsan Raghunathan[1]*

[1]Institute of Bioinformatics and Applied Biotechnology (IBAB), Biotech Park, Electronic City Phase I, Bengaluru 560 100, Karnataka, India.

[2] Manipal Academy of Higher Education, Manipal, 576104, Karnataka, India.

* srivatsan@ibab.ac.in

+ These authors contributed equally to this work

Abstract

Background

Osteoclast differentiation in the inflamed synovium of Rheumatoid Arthritis affected joints leads to the formation of bone lesions. Reconstruction and analysis of protein interaction networks underlying specific disease phenotypes are essential for designing therapeutic interventions. In this study we have created a network that captures signal flow leading to osteoclast differentiation. Based on transcriptome analysis, we have indicated the potential mechanisms responsible for the phenotype in the Rheumatoid Arthritis affected synovium.

Method

We collected information on gene expression, pathways and protein interactions related to Rheumatoid Arthritis from literature and databases namely Gene Expression Omnibus, KEGG pathway and STRING. Based on these information, we created a network for the differentiation of osteoclasts. We identified the differentially regulated network genes and reported the signaling that are responsible for the process in the Rheumatoid Arthritis affected synovium.

Result

Our network reveals the mechanisms underlying the activation of the Neutrophil Cytosolic Factor complex in connection to osteoclastogenesis in Rheumatoid Arthritis. Additionally, the study reports the predominance of the canonical pathway of NF-κB activation in the diseased synovium. The network also confirms that the upregulation of T cell receptor signaling and downregulation of TGFβ signaling pathway favour osteoclastogenesis in Rheumatoid Arthritis.

To the best of our knowledge, this is the first comprehensive protein-protein interaction network describing Rheumatoid Arthritis driven osteoclastogenesis in the synovium.

Discussion

This study provides information that can be used to build models of the signal flow involved in the process of osteoclast differentiation. The models can further be used to design therapies to ameliorate bone destruction in the Rheumatoid Arthritis affected joints.

Introduction

Rheumatoid arthritis (RA) is a systemic autoimmune disease that primarily affects synovial joints. The disease is characterised by chronic inflammation in the joints, leading to synovial hyperplasia (pannus formation), destruction of the cartilage and erosion of the underlying bone. RA is a complex disease involving several molecular pathways across various cell types and tissues. Thus in order to elucidate the underlying cause of a particular phenotype associated to the disease, identification of the network consisting of differentially expressed genes (DEG) in the interacting pathways is essential. Studies have used pathway analysis to identify affected pathways from lists of DEGs (Hao et al., 2017; Wang et al., 2017; Lee et al., 2011; Wu et al., 2010). The lists have also been used to create networks that are related to specific diseases or conditions. Earlier work using RA samples has focused on generating networks of the genes showing differential regulation (Hao et al., 2017; Wang et al., 2017) or the most enriched gene ontology (GO) ("Expansion of the Gene Ontology knowledgebase and resources.," 2017) category in the DEG lists (Lee et al., 2011). A comprehensive network describing molecular interactions across various RA affected tissues was created using publicly available microarray data by Wu *et al* (Wu et al., 2010). Other groups have created gene regulatory networks (GRN)

using *in vitro* data from cultured fibroblasts and macrophages (Kupfer et al., 2014; You et al., 2014). Kupfer *et al* (Kupfer et al., 2014) used time series data generated from RA synovial fibroblasts subjected to external stimulation to create a GRN. They simulated the network to analyse the behaviour of genes involved in RA pathogenesis, in response to stimulation by RA associated cytokines and growth factors. You *et al* (You et al., 2014) created a GRN and identified the critical interactions responsible for synovial fibroblast invasiveness in RA synovium. The creation of a detailed protein-protein interaction (PPI) network describing the connections between various pathways involved in any specific RA process, at the level of the synovial tissue, is yet to be attempted. In this study, using the publicly available gene expression data for RA synovial tissue and protein interactions and pathway databases, we created and analysed a detailed phenotype-specific PPI network. We used differentially regulated genes to identify the altered pathways in the affected synovium. We identified the pathway of osteoclast differentiation as a phenotype connected to many of the altered pathways in the RA synovium. It is established that the RA synovium harbors osteoclasts, the cells responsible for bone degradation in the affected joints (Schett, 2007). Therefore, a network of proteins participating in the interacting pathways underlying the RA associated process of osteoclast differentiation in the synovium was created for the first time. We report the upregulated signaling routes that drive osteoclastogenesis via the generation of reactive oxygen species (ROS) by Neutrophil Cytosolic Factor (NCF) complex in the RA synovium. We demonstrate the contribution of elevated T cell receptor signaling in facilitating osteoclast differentiation in the affected tissue. In addition, we describe the importance of the canonical pathway of NF-κB activation and the TGFβ pathway in connection to the process. Finally, the network reports all the possible routes by which the inflamed synovium promotes the differentiation of osteoclasts.

Materials and Methods

This study involved two major steps: selection of a phenotype exhibited by the RA synovium, and construction and analysis of a PPI network for the selected phenotype. Figure 1 shows the detailed workflow that was followed. Each step is described in detail in this section. The databases used in this study are summarized in Table 1.

Identification of DEGs using microarray data analysis

The DEGs were obtained by re-analysing the publicly available microarray datasets in Gene Expression Omnibus (GEO) (Edgar, Domrachev & Lash, 2002) database. The repository was searched for the data generated from synovial tissue in RA patients and healthy controls. The results were further narrowed down by considering only the data from Affymetrix platforms with at least four RA and four control samples. Datasets selected for the study are mentioned in Table 2.

Of the seven datasets, information regarding treatments received by the patients was not available for GSE77298 (Broeren et al., 2016) and GSE7307. Earlier, it was established that the differential regulation of the genes in these datasets was not under the influence of drug therapy (Dey, Panga & Raghunathan, 2016). The clinical information for the RA patients was available for the datasets GSE1919 (Ungethuem et al., 2010), GSE12021 (U133A) (Huber et al., 2008), GSE12021 (U133B) (Huber et al., 2008), GSE55235 (Woetzel et al., 2014) and GSE55457 (Woetzel et al., 2014). The erythrocyte sedimentation rate (ESR) and the concentration of C-reactive protein (CRP) reported for these datasets were higher than 40 mm $hour^{-1}$ and 21 mg $litre^{-1}$ respectively. These values indicated active inflammation in the synovium of the RA patients

(Wetteland et al., 1996 ; Otterness, 1994). For the datasets, GSE77298 and GSE 7307, the values for these parameters were not available.

Raw data from the seven datasets along with their metadata was downloaded using the R libraries GEOquery (Davis & Meltzer, 2007) and GEOmetadb (Zhu et al., 2008). The data was analysed using the affy (Gautier et al., 2004) and simpleaffy (Wilson & Miller, 2005) libraries in the Bioconductor package in R (R Core Team, 2017).

In this analysis, two algorithms, Robust Multiarray Average (RMA) and Microarray Suite 5.0 (MAS5) were used for the data normalization. The choice of data normalization algorithms affect the final selection of the DEGs (Pepper et al., 2007). In order to reduce the algorithm specific effects, both RMA and MAS5 were used in this study. In the case of MAS5, probesets having at least one present call ("P") in control as well as treatment samples were considered. Probesets were annotated with Entrez IDs using the Bioconductor as well as DAVID gene-ID conversion tool (Huang, Sherman & Lempicki, 2009b; Huang, Sherman & Lempicki, 2009a). Welch t test was applied to calculate the significance for differential expression between the RA and the control samples. As per the recommendations by Huang *et al* (Huang, Sherman & Lempicki, 2009a), in our study a gene with a linear fold change of 2 (for up and downregulation) and a p value <= 0.05 was considered to be differentially expressed. A final list of DEGs, from the seven datasets, was obtained using the selection rules as described below:

A. In a dataset, a gene is considered to be upregulated if:

i. It is upregulated in both RMA and MAS5 [+,+]

Or,

ii. It is upregulated in one of the algorithm and not differentially expressed in the other [+, 0] or [0, +].

B. Across the datasets, the gene is upregulated if:

i. It is [+, +] in at least one of the seven datasets and no downregulation in any of the datasets

Or,

ii. It is [+, 0], in at least one dataset and [0, +] in at least one of the remaining datasets while there is no downregulation in any one of them

The same procedure was repeated for the downregulated genes.

When the selection criteria was made more stringent by demanding the selection of a gene in at least two datasets, the number of selected genes reduced by almost 50 percent as shown in Fig. 2. Since the aim of the study was to identify all the important signaling associated with the RA-associated process we decided to proceed with the selection criteria of presence in at least one dataset.

Finally, we prepared a list of up and downregulated genes which we named as “common-up” and “common-down” respectively.

Pathway Analysis:

The common-up and common-down gene lists were separately examined for the enrichment of pathways listed in the Kyoto Encyclopedia Of Genes And Genomes (KEGG) database (Kanehisa et al., 2017) using Database for Annotation, Visualization and Integrated Discovery (DAVID). For the enrichment analysis, we created a custom background by combining the total probesets present on all four microarray platforms and annotating them with Entrez IDs using the DAVID gene ID conversion tool. The pathways which were significantly over-represented in the common-up or common-down gene lists with an EASE score <= 0.05 and fold enrichment >=

1.5 were considered to be affected in RA (Huang, Sherman & Lempicki, 2009a). EASE score is a modified one-tailed Fisher exact probability used in enrichment analysis (Hosack et al., 2003).

The pathways were grouped according to their KEGG categories. Those belonging to the categories “human diseases”, “metabolism” or the ones lacking protein-protein interactions were not considered further. The category “human diseases” contains pathways that represent specific disease conditions. These were excluded because they do not reflect the protein-protein interaction in healthy conditions. “Metabolism” contains pathways that describe interconversions of metabolites. Since this study focused on PPI involved in the RA affected synovium, we did not consider the metabolic pathways. The remaining pathways were categorized based on their functional specificity. The pathways which result in a specific function like platelet activation were tagged as process pathways, whereas the pathways describing more general signaling events like the activation of multiple transcription factors through T cell receptor signaling, were considered as signaling pathways.

The list of genes present in each selected pathway was downloaded from KEGG using the KEGGREST (Tenenbaum, 2017) package in R. For each one of the selected pathway, the list of genes that were common between the pathway and the microarray platforms was created. We name this as “S-list”. By the pairwise intersection of the S-list of each process pathway with every one of the non-disease pathway, we obtained the DEGs shared between the pairs of process and non-disease pathways. The number of DEGs shared by each pair was examined. The pairs of pathways sharing at least five upregulated or five downregulated genes were retained for our study. Figure 3 shows the number of up or downregulated genes common to the pair of pathways. It is evident from this figure that the above mentioned criterion did not result in a bias towards pairs of larger pathways.

Construction of network:

We constructed a PPI network for the osteoclast differentiation. The osteoclast differentiation pathway (ODP) proteins, obtained from KEGG were defined as a set of core proteins. Interactors of the core proteins (first-shell interactors) were extracted from the STRING database (version 10) (Szklarczyk et al., 2015). The protein list was restricted by considering only experimentally validated interactions with a score of >= 0.9. This score on a scale of 0 to 1 represents the confidence of experimental validation with maximum confidence being 1. We obtained the directions for these interactions from the literature references used in STRING, when available, or with a separate literature search in Pubmed. The complete network was built in Cytoscape (Shannon et al., 2003) using all the obtained interactions. The proteins corresponding to the DEGs in RA synovium obtained from the microarray data analysis were indicated in this network.

Analysis of the network:

The network was a mixed network consisting of the undirected protein binding edges and the directed edges of activation, inhibition or the post-translational modification (PTM). The nodes are labelled using the official gene symbols corresponding to the proteins used to create the network. The interactions involved undirected protein-protein interactions or directional PTM like phosphorylation, methylation, acetylation, ubiquitination *etc.* We included activation or inhibition as an interaction whenever the reference mentioned that the target protein is activated or inhibited as a result of the interaction. We created a version of this directed network without UBC and its edges. We named this version as “directed ODP network”.

We conducted GO enrichment analysis on the directed ODP network proteins using the GO molecular function (GOMF) and GO biological process (GOBP) terms. Terms with an EASE score <= 0.05 and fold enrichment >=1.5 were considered as enriched. We combined 23 enriched GOMF terms to identify the proteins that bind to DNA. In the case of the GOBP terms, we selected the enriched signaling terms that contained differentially regulated genes for T cell receptor signaling, B cell receptor signaling and FC-ε receptor signaling. For NF-κB signaling, TLR signaling and TGFβ signaling pathways we combined six, nine and three enriched terms respectively and examined their differential regulation. Using the selected enriched signaling terms, we extracted subnetworks corresponding to each signaling pathway from the directed ODP network. All the subnetworks demonstrate the flow of information from the first-shell interactor proteins to the core proteins of the ODP network. The details of the GOMF and GOBP signaling terms enriched in the analysis is provided in the Tables S1 and S2 respectively.

The database DrugBank (Wishart et al., 2018) was explored to locate the target proteins of drugs that are commonly used in the treatment of RA. We used the information to pinpoint the network proteins which are targets of the RA drugs. The details regarding the drugs and their targets are submitted in Table S3.

We converted all the edges of the directed ODP network to single undirected protein binding edges to create an "undirected ODP network". We analysed this network using the Cytoscape plugin NetworkAnalyzer (Assenov et al., 2008). We used the plugin MCODE v1.5.1. (Bader & Hogue, 2003) to identify the clusters in the network.

Results

Differentially expressed genes in RA synovium

We analysed seven Affymetrix microarray datasets from five different platforms. Out of 21,246 Entrez annotated genes measured, 1018 upregulated and 893 downregulated genes were identified in the RA synovium compared to the healthy controls. The differentially regulated genes are submitted in Table S4. Only three genes STAT1, IL7R and IGKC were upregulated in all seven datasets. Interestingly, three AP1 proteins FOSB, JUN and JUNB were downregulated. Table 3 shows the datasets in which the genes were downregulated.

Diverse pathways are involved in the disease processes affecting the RA synovium

Using the DEGs from the microarray analysis as the input, we found that 52 KEGG pathways were enriched in the upregulated gene list, and 29 in the downregulated gene list. The EASE scores of the selected pathways were much less that the cut-off of 0.05. The enrichment analysis when performed with the combined DEG list (1018 up genes + 893 down genes) resulted in only 55 pathways. Among these, only two pathways were newly obtained when compared to the previous list of 52 upregulated and 29 downregulated pathways. As the combined analysis proved less informative, the 52 up and 29 downregulated pathways were considered for the study. Three pathways, namely, Extra cellular matrix (ECM)-receptor interaction, Focal adhesion and Proteoglycans in cancer occurred in both the up and downregulated pathway lists because each pathway had a significant number of up and downregulated genes. The KEGG category-wise distributions of the enriched pathways are shown in Fig. 4 and Fig. 5 and the detailed results of the pathway analysis are given in the Table S5 and S6. 26 of the upregulated pathways and four of the downregulated pathways belonged to the KEGG category “human diseases”.

Among the upregulated non-disease pathways, the category “immune system” had the highest number of enriched pathways. Most of the immune receptor signaling pathways in this category were upregulated. Among the other signaling pathways, NF-κB and JAK-STAT signaling

pathways were upregulated in our analysis. All the signaling pathways which belong to the KEGG categories, "immune system" and "signal transduction" that were enriched in the upregulated gene list are shown in Table 4.

Specialized cells called osteoclasts which facilitate bone resorption are also present in the invading pannus of the RA joints (Gravallese et al., 1998; Jung et al., 2014; Nevius, Gomes & Pereira, 2016). All the five microarray datasets which provided information on the disease state, GSE1919, GSE12021 (U133A), GSE12021 (U133B), GSE55235 and GSE55457, used tissue from patients with more than ten years of disease. Patients from the other dataset GSE77298, were at the end stage of the disease. Since osteoclast differentiation is reported in severely inflamed RA synovium, the process is likely to be detected in the synovial tissue used for the datasets. It is noteworthy that our analysis identified the pathway osteoclast differentiation as one of the enriched pathways with a fold enrichment of 3.11 (EASE score of 2.41 e^{-8}) in the RA synovium. In addition, our analysis detected the upregulation of two well-known osteoclast markers Cathepsin K (CTSK) and tartarate resistant acid phosphatase (ACP5) in the synovium.

The category highly represented in the list of downregulated pathways was "signal transduction". All the signal transduction pathways enriched in the downregulated gene list are given in Table 5. In contrast to the upregulated pathways, the downregulated pathways included several metabolic pathways such as fatty acid degradation, fatty acid elongation *etc.* Some endocrine system pathways like regulation of lipolysis in adipocytes, insulin signaling pathway, which are closely related to metabolic regulation were also listed among the downregulated pathways.

RA affected signaling pathways interact to orchestrate osteoclast differentiation in the synovium

We categorised the 26 upregulated and 25 downregulated non-disease pathways based on their functional specificity. In this analysis we identified 12 process pathways and 19 signaling pathways among the differentially regulated pathways. This list of 31 pathways includes the process pathway focal adhesion which was differentially regulated in both directions. While four and ten process and signaling pathways respectively were downregulated, nine process and signaling pathways each were upregulated. The detailed information about the number of upregulated, downregulated and total genes in each of the selected pathway is submitted as Table S7 and S8.

We examined the overlap of the process pathways with all the non-disease pathways based on the shared number of DEGs. The overlapping pathways are represented as a pathway interaction network in Fig. 6. Several of the signaling pathways share DEGs with the process pathways indicating that the process is influenced by these signaling pathways. The details of the DEGs shared by each pathway pair is presented in the Table S9.

Figure 7 is a graphical representation of the number of genes shared between the Osteoclast differentiation pathway and other non-disease pathways. Signaling pathways, represented by light blue bars, constitute eight out of the 13 non-disease pathways that interact with osteoclast differentiation. All the pathways sharing genes with osteoclast differentiation pathways are upregulated pathways. Similar graphs were created for all upregulated process pathways and are available in the supplementary figures: Fig. S1 - Fig. S7. Figure 8 shows the overlap analysis for the downregulated signaling pathways.

Among the downregulated process pathways shown in Fig. 8, vascular smooth muscle contraction interacted with platelet activation and cGMP-PKG signaling pathway, via downregulated genes in the RA synovium. Regulation of lipolysis in adipocytes interacted only

with down signaling pathways through downregulated genes. Finally, the pathway adherens junction did not overlap with any other pathways.

Our study revealed that the processes of natural killer cell mediated cytotoxicity as well as osteoclast differentiation involved a network of several interacting pathways in the RA synovium. However, osteoclast differentiation was influenced by the highest number of signaling pathways. This indicates that the differentiation of osteoclasts in the RA synovium is coordinated by several signaling pathways. In order to understand the collective effect of these signaling pathways on the osteoclast differentiation, we created a detailed PPI network for the process in the RA synovium. Among all the interactions obtained from the STRING database, we used only the experimentally validated ones published in literature, for the creation of the network. In this network, we indicated the differentially regulated genes from the microarray analysis to show the possible ways by which the altered signaling promotes osteoclastogenesis in RA synovium.

A comprehensive PPI network for the differentiation of osteoclasts in RA synovium

The PPI network, created in our study, had 433 proteins and 1790 interactions. The network consisted of three connected components. The two smaller connected components were the interactions between CD47 and SIRPA, and IL1A and S100A13.

The protein Ubiquitin which has the highest number of interactions in the network was found to interact with 175 network proteins. This is expected, as ubiquitination is a very common PTM that marks the proteins for proteasomal degradation. In our network, ubiquitination was represented as interaction of a protein with ubiquitin as well as with ubiquitin ligases. We removed ubiquitin from our network since most of the edges of ubiquitin and those of the ubiquitin ligases were redundant. The resulting network had 432 proteins and 1595 interactions.

297 In this network, in addition to the two small connected components, four proteins, PPP3R1,
298 PPP3CA, PPIA and RCAN1 were disconnected from the main network and formed a new
299 connected component. The network now had four components: CD47-SIRPA, IL1A-S100A13,
300 PPP3R1-PPP3CA-PPIA-RCAN1, and one large component.

301 We removed the three smaller connected components from the main network. The large
302 connected component, consisting of 424 protein nodes and 1589 interactions, was used for
303 further analysis. Henceforth, we refer to this as directed ODP network. The directed ODP
304 network contains 82 core proteins belonging to the KEGG osteoclast differentiation pathway.
305 The portion of the directed ODP network containing the 82 core proteins and their 152
306 connections is termed as the "**core network"** (directed). The rest of the network consisting of the
307 first shell interactors and their edges is the **"shell network"** (directed). The core network
308 contains proteins which are directly involved in the osteoclast differentiation. The shell network
309 represents the protein milieu in the RA synovium facilitating the osteoclast differentiation. The
310 complete directed ODP network is provided as a supplementary file S1. A second supplementary
311 file S2 contains the information about the core and shell proteins of the ODP network.

312 **The DNA-binding proteins of the directed ODP network**

313 In a PPI network, the terminal responders of the signals are the DNA-binding proteins such as a
314 transcription factors (TF), coactivator *etc*. or the proteins that generate non-protein signaling
315 molecules like secondary messengers. Using the enriched terms in the category GOMF, we
316 classified 82 of the 424 nodes as DNA-binding proteins (Fig. S8). 18 DNA- binding proteins
317 which include STAT, NF-κB and AP1 TF belong to the core network. Along with the differential
318 expression of STAT1, JUN, JUNB and FOSB, the STAT protein STAT2 was upregulated in this
319 study.

In addition to STAT and AP1 proteins, the other DNA binding core protein PPARG was observed to be downregulated which is in agreement with the results of Li *et al* (Li et al., 2017). The attachment of the shell network resulted in the inclusion of nine differentially regulated DNA-binding proteins in the directed ODP network. The possible roles of these proteins in osteoclastogenesis are described in context of their GOBP terms.

The signaling pathways of the directed ODP network

GOBP over-representation analysis of the directed ODP network proteins identified several immune signaling terms. These terms included five out of the eight upregulated KEGG signaling pathways which were found to interact with the osteoclast differentiation (Fig. 7). These pathways are: T cell receptor signaling pathway, B cell receptor signaling pathway, Fc-ε receptor signaling pathway, NF-κB signaling pathway and Toll-like receptor (TLR) signaling pathway.

Among these, T cell receptor signaling pathway had the most number of DEGs, with 14 up and one downregulated nodes. The proteins belonging to the T cell receptor signaling term were extracted as a subnetwork (Fig. S9). In this subnetwork, the T cell surface molecules CD3E and CD28 were upregulated whereas CD247 did not show differential regulation. The downstream signaling molecules ZAP70, LCK, ITK, CSK, LAT, LCP2, FYB, PAG1, PIK3CD, MAPK1, PLCG2 and INPP5D were upregulated. Among them, PIK3CD, MAPK1, LCK, LCP2 and PLCG2 are the core network proteins.

The B cell receptor signaling pathway (Fig. S10) term shared six proteins with the core network. Five of these core proteins were upregulated. In addition, ZAP70, LYN and PRKCB, which are part of the shell network, were found to be upregulated.

The Fc-ε receptor signaling pathway (Fig. S11) showed the MAP Kinase, NF-κB, Rac signaling components. The term showed nine upregulated genes which included the receptor FCER1G.

Six GOBP terms were combined to extract 75 proteins of the NF-κB signaling pathway from the directed ODP network (Fig. S12). This NF-κB subnetwork contained five receptors including one core protein (TNFRSF1A). Out of the 11 DEGs in the subnetwork, TNFSF11 (RANKL) and STAT1 were the core proteins. REL, a component of NF-κB transcription factor dimers was upregulated. The osteoclast differentiation and activation factor, RANKL, an activator of NF-κB pathway was highly upregulated with a log2 fold change of 3.32. It is known that REL participates in the canonical NF-κB signaling (Shih et al., 2011). Of the many possible signaling routes leading to REL, we observed DEGs in the following pathways: TCR-PRKCQ-CARD11-BCL10; IL1R1-MyD88-IRAK4; TNFSF11 (RANKL)-TRAF6-IKK; CD27-TRAF2-IKK. We have extracted all these routes and created a subnetwork for activation of REL in the RA synovium (Fig. 9).

We combined nine over-represented GOBP terms to extract the TLR signaling pathway proteins (Fig. S13). The extracted subnetwork featured the signaling from the receptors TLR3 and TLR4 to the IκB kinase complex (IKK). Although the pathway is upregulated in the RA synovium, the TLR receptors in the ODP network did not show any differential regulation.

Interestingly, the directed ODP network demonstrated a downregulation of all the DEGs participating in the TGFβ signaling pathway. The TGFβ subnetwork (Fig. S14) showed the presence of the ligands TGFB1, TGFB2 and TGFB3 and the receptors TGFBR1, TGFBR2 and TGFBR3. Among the downstream SMADs, SMAD3 was downregulated.

Protein clusters in the directed ODP network

The analysis done using the MCODE application of the Cytoscape tool revealed 19 clusters which may indicate functional protein complexes. The details of these 19 clusters are submitted as Table S10. Among them, 12 clusters included a mixture of core and shell proteins. In three of the clusters (Cluster2, Cluster 4 and Cluster 10), the core proteins were differentially regulated. Cluster 2 comprised of three core proteins and six shell proteins. The cluster had two DEGs which were DNA-binding proteins STAT1 and PPARG. Cluster 4 was a TGFβ cluster and cluster 10 was an NCF cluster. The TGFβ cluster had two downregulated proteins, of which SMAD3 was a shell protein. The NCF cluster had four core proteins, of which NCF2, NCF4 and CYBA were upregulated. The upregulated shell protein in the NCF cluster was NCF1.

Discussion

This study is aimed at understanding the mechanisms involved in a specific RA-related phenotype. We have used a large number of microarray studies and relaxed inclusion criteria for differential expression across datasets, to obtain relatively large number of DEGs that are likely to be involved in RA. We have combined this gene expression data with pathway analysis and identified various process pathways and several signaling pathways to be affected by RA. In systemic diseases like RA, pathways responsible for a particular phenotype operate in an environment consisting of various other disrupted pathways. Thus it becomes important to understand the effect of this environment on the pathway immediately responsible for the phenotype. We attempted to achieve this by overlapping the various process pathways with the enriched signaling pathways in the synovium. Interestingly, the process pathway osteoclast differentiation overlapped with several of the enriched signaling pathways. In order to understand the signaling involved in osteoclast differentiation in the RA synovium, for the first

time, we created a detailed PPI network responsible for the phenomenon. Each interaction in this network was manually verified from literature enabling the inclusion of directions of the interactions and specific post translational modifications whenever such information was available. While creating the network using all the possible interactions available in STRING, we found that some proteins in the repository have more number of interactions reported than the others. We acknowledge that this might have led to a bias in the directed ODP network. The network lacks the important non-protein molecules involved in triggering the ectopic differentiation of osteoclasts in the inflamed synovium. In addition, gene expression regulation resulting from activation or repression of transcription factors was not depicted in the network. Since the RA specific data used in this network was only gene expression data, information on the activation state of specific proteins that are known to be involved in the disease, e.g., phosphorylation state of STAT1 was missing. Though the network lacks these information, it is the most comprehensive and informative PPI network till date describing the process of osteoclast differentiation.

The differentially regulated genes in the RA synovium

In order to identify the DEGs in the RA synovium, seven microarray datasets generated by five different studies were used. Among the seven datasets, the RA patients belonging to the datasets GSE1919, GSE12021 (U133A), GSE12021 (U133B), GS55235 and GSE55457 had similar high values for the inflammatory markers, ESR and CRP. Additionally, the tissue used in GSE77298 were described as end stage RA synovial biopsies. Therefore, we surmise that the RA tissues were highly inflamed. However, we observed that few genes were differentially expressed across most of the datasets (Fig. 2). Since the level of inflammation in RA tissues were comparable, we attribute this lack of concordance between the datasets to the heterogeneity of the disease.

The enriched pathways in the RA synovium

KEGG pathway enrichment analysis of the upregulated genes (common-up) resulted in 26 upregulated disease pathways. As expected, Rheumatoid arthritis was one of these disease pathways. Staphylococcus aureus infection and Tuberculosis, the two upregulated infectious disease pathways in the results of the pathway enrichment analysis are known to be associated with RA (Sams et al., 2015; Jeong et al., 2017). The upregulated infectious disease pathways share several genes with immune system pathways. Differential regulation of the immune pathways is expected in RA since it is an immune disorder. Therefore, the upregulation of the immune genes explains the enrichment of the infectious disease pathways in the up pathway list.

Several pathways belonging to the category "immune system" were enriched in the common-up genes. The enrichment of these immune pathways is likely as infiltration of activated immune cells has been observed in the RA synovium (McInnes & Schett, 2011). In addition, the resident cells of the inflamed pannus exhibit activation of several immune signaling pathways (McInnes & Schett, 2007). Among the pathways from Table 4, the Fc-ε RI signaling pathway shows an upregulation of the IgE receptor Fc-ε RI. Elevated presence of IgE and activated mast cells have been detected in the RA synovium (Gruber, Ballan & Gorevic, 1988; Tetlow & Woolley, 1995). It has been demonstrated by *in vitro* experiments that the RA synovial mast cells express Fc-ε RI and can be activated via the Fc-ε RI signaling pathway (Lee et al., 2013). However, the contribution of the pathway to the pathological alteration of synovial tissue function needs to be addressed in future studies.

Among the enriched downregulated pathways, seven belong to the category "signal transduction" (Table 5). The AMPK signaling pathway which is known for its anti-inflammatory effect shows downregulation in our analysis (Speirs et al., 2018). The downregulation of the

FOXO signaling pathway is also observed in this study. This reflects the results of the earlier studies which have shown downregulation and inactivation of the FOXO transcription factors in the RA affected synovium (Ludikhuize et al., 2007; Grabiec et al., 2015). Additionally, the FOXO proteins are inhibited by NF-κB signaling, and activated by AMPK as shown in the FOXO signaling pathway listed in KEGG pathway database. The pathway enrichment results from our analysis show upregulation in NF-κB signaling and downregulation in AMPK signaling, which explains the downregulation of FOXO signaling. Further, the cGMP-PKG signaling is known to be essential for the vascular smooth muscle response to the inflammatory cytokines (Browner, Sellak & Lincoln, 2004). The downregulation of genes in this pathway needs to be studied in detail to analyse the effects of RA synovial inflammation on the blood vessels in the affected tissue. The cAMP signaling pathway is known to facilitate regulatory T cell function and T cell anergy (Raker, Becker & Steinbrink, 2016). The downregulation in this pathway might indicate the pro-inflammatory nature of the infiltrating T cells in the synovium. It is difficult to explain the importance of downregulation in the Wnt signaling pathway and the MAPK signaling pathway in the RA synovium. Wnt signaling, which is required for repair of bone erosions, is suppressed in mouse models of inflammatory arthritis (Lories, Corr & Lane, 2013). However, Wnt signaling has also been linked to proinflammatory cytokine production in the affected synovium (Miao et al., 2013). In our study, the KEGG Wnt signaling pathway is enriched in downregulated genes. Among the downregulated genes, two are Wnt receptors FZD4 and LRP6, whereas three are the Wnt antagonists SFRP1, SFRP2 and SFRP. Thus no conclusions can be made about the role of Wnt signaling pathway from its presence in the list of downregulated pathways. Similarly, no clear picture can be drawn about the role of MAPK signaling pathway in the RA synovium. This is because the KEGG MAPK signaling pathway is

very large, with 252 genes and several genes are grouped together under terms like RTK (receptor tyrosine kinase) and GF (growth factor), making the pathway extremely general.

Construction of the directed ODP network

Three small connected components were removed while creating the directed ODP network. One of the components contained the proteins PPP3R1 and PPP3CA which are the subunits of calcineurin, an important regulator of osteoclast differentiation. The immunosuppressant drug cyclosporin used in the treatment of RA acts as an inhibitor of calcineurin by forming a ternary complex with PPIA and calcineurin (Wang & Heitman, 2005). The remaining protein in the connected component, RCAN1 is an inhibitor of calcineurin. Both in the KEGG pathway database and in literature, these proteins are described as participating in the RANKL signaling pathway which regulates the differentiation of osteoclasts. Calcineurin participates in the RANKL signaling pathway downstream of the non-protein components inositol triphosphate and calcium ions. Since our network is based on protein-protein interactions, it failed to capture the connection of calcineurin and its adjacent proteins to the large connected component, in spite of showing the connections of other RANKL pathway proteins.

Analysis of the directed ODP network

The directed ODP network was analysed to examine three main aspects. Firstly, the proteins binding to DNA were explored because they are involved in regulating gene expression. Secondly, the proteins involved in signal transduction were studied for their role in facilitating the process of osteoclast differentiation in the RA affected synovium. Finally, the clusters of highly interconnected proteins were identified in the network. Several proteins function as part of protein complexes. The protein clusters we identified may represent the protein complexes. We also examined the differential expression of the proteins in the clusters. Protein clusters with

differentially regulated proteins may represent complexes actively involved in the osteoclastogenesis in RA synovium.

DNA binding proteins in the directed ODP network

Among the DNA-binding proteins in the directed ODP network, the downregulation of the AP1 proteins JUN and JUNB is in contrast to the earlier studies which reported their upregulation in RA synovium (Kinne et al., 1995). As shown in Table 3, the AP1 downregulation was observed in five of the seven datasets, with the three proteins FOSB, JUN and JUNB being downregulated in three out of the seven datasets. The presence of consistent downregulation in the datasets from different studies shows that the downregulation of these proteins is not due to dataset specific factors. As mentioned earlier, four of the five datasets showing downregulation had patients with similar clinical characteristics. This may suggest a connection between the stage of the disease and the downregulation of the AP1 proteins. Further studies are required to explain the downregulation of these AP1 proteins in the synovium of a subset of RA patients.

According to previous reports, another AP1 protein FOS is upregulated in the RA synovium (Dooley et al., 1996). However, our analysis does not show any differential regulation of FOS. FOS is an indispensable transcription factor for osteoclast differentiation (Grigoriadis et al., 1994). In the ODP network, the upregulation of MAPK1 and RPS6KA1 presents a possible mechanism for FOS activation. In addition, our network reveals the activation of FOS by the upregulated TF STAT1. Along with STAT1, the TF STAT2, the kinase JAK2 and the receptor IFNAR2 were upregulated in the IFN pathway of the ODP network. TNFSF11 (RANKL) induces expression of IFNβ which serves as a feedback inhibitor of osteoclastogenesis via STAT1 (Xiong et al., 2016). The upregulation of the IFNβ receptor, IFNAR2 and the TF STAT1 may indicate that the feedback inhibition is functional in the RA synovium.

Signaling pathways in the directed ODP network

The examination of the enriched GOBP terms of the network showed an involvement of T cell receptor signaling pathway, B cell receptor signaling pathway, Fc-ε receptor signaling pathway and NF-κB signaling pathway in the differentiation of osteoclasts in the RA synovium. Figure 9 depicts the signaling routes that lead to activation of REL in the RA synovium. The figure shows activation of REL by PKC. The network shows T cell receptor mediated activation of PRKCQ and its subsequent activation of CARD11. Based on earlier studies (Szamel, Bartels & Resch, 1993; Sommer et al., 2005), we speculate that another isoform of PKC, PRKCB is also involved in the activation of CARD11 in the affected synovium. It is known that the activated CARD11 via the formation of a trimeric complex with BCL10 and MALT1 activates the IKK complex (Turvey et al., 2014). The IKK complex in turn activates NF-κB proteins including REL by removing their inhibition by NFKBIA and NFKBIB. Figure 9 shows that the ODP network has captured the interactions of these proteins. In this pathway, the upregulation of PRKCB and REL and the downregulation of NFKBIA indicate activation of REL via this pathway in the RA affected synovium. It is also known that NF-κB proteins are activators of RANKL (TNFSF11) gene expression in activated T cells (Fionda et al., 2007). Our network, through the presence of DEGs in the RA synovium, shows how TCR signaling aids in activation of REL which leads to RANKL expression and osteoclastogenesis. In addition, the upregulation of TNFSF11 and downregulation of its competitive inhibitor TNFRSF11B marks another route to the activation of REL via TRAF6. PPARG, a known inhibitor of TNFSF11-mediated osteoclastogenesis, was downregulated in the ODP network. This result agrees with the findings of Li *et al* (Li et al., 2017). The upregulation of CD27 receptor is in accordance with the reports of high levels of CD27 in the synovial tissue of RA patients (Tak et al., 1996). As CD27 also activates TRAF6,

523 we speculate that the upregulation of CD27 contributes to the activation of REL via this route in
524 the RA synovium. Among the DEGs involved in the REL activation via IL1 pathway, CASP1
525 was upregulated whereas the inhibitor PELI1 was downregulated. This is balanced against the
526 upregulation of IL1RN, a competitive inhibitor of IL1R1. It is known that both the cytokines,
527 IL1 and TNF, activate NF-κB through TRAF6. However, we did not observe differential
528 regulation of the TNF pathway proteins leading to the activation of NF-κB. On the other hand,
529 the apoptosis related proteins such as FAS and CASP8 which are downstream to TNF receptor,
530 were upregulated. Earlier studies have established that the death signaling pathways are
531 antagonized by the activity of BIRC2, BIRC3 and XIAP (Vasudevan & Ryoo, 2015). The
532 upregulation of BIRC3 points to suppression of TNF mediated apoptosis and the activation of
533 NF-κB via TNF receptor signaling in the RA synovium. This reflects the possibility that TNF
534 signaling results in both CASP8 mediated apoptosis and BIRC3 mediated NF-κB activation in
535 different parts of the RA synovium. The network also captures the activation of IKK by the
536 upregulated NOD2 through MAP3K7. Studies have reported that RA synovial cells express high
537 levels of NOD2 (Franca et al., 2016). We hypothesize that NOD-dependent activation of NF-κB
538 also contributes to the osteoclastogenesis in RA synovium. All the routes that lead to activation
539 of NF-κB points to the canonical signaling. PEL1 is known to be a negative regulator of REL
540 (Chang et al., 2011). REL, which functions only in the canonical NF-κB pathway, is the only
541 NF-κB protein showing differential regulation in this analysis (Shih et al., 2011). The
542 upregulation of REL, BIRC3 and PRKCB and the downregulation of PELI1 also support the
543 predominance of canonical NF-κB signaling in RA synovium osteoclastogenesis (Lutzny et al.,
544 2013; Varfolomeev et al., 2007).

The GOBP analysis revealed enrichment of TGFβ signaling pathway terms. The role of TGFβ signaling pathway in osteoclastogenesis is not captured in the KEGG osteoclast differentiation pathway as it shows only the receptor-ligand interaction. Our network connects the TGFβ receptors to downstream DNA-binding proteins, of which Forkhead box proteins, SMAD3 and ATF3 were downregulated. The consistent downregulation of all the DEGs in the TGFβ pathway implies their negative regulatory role in the osteoclastogenesis. Although the published studies support a mixed role of TGFβ pathway in the RA synovium, Karst *et al* showed that high concentration of TGFβ is involved in the inhibition of osteoclastogenesis (Karst et al., 2004). Therefore, we hypothesize that the downregulation of the TGFβ pathway produces a favourable environment for osteoclastogenesis in the RA synovium.

A proposed model of enhanced ROS production mediating osteoclastogenesis in RA synovium

It is known that the Nox2 complex generates ROS which act as secondary messengers during osteoclast differentiation (Kang & Kim, 2016). ROS are also known to cause activation of canonical NF-κB pathway (Gloire, Legrand-Poels & Piette, 2006). In the ODP network, the upregulation of NCF1, NCF2, NCF4 and CYBA, the four components of Nox2 complex, may indicate the osteoclast differentiation as well as oxidative burst by phagocytic cells in the RA synovium (Rosen et al., 1995). The NCF cluster, selected by MCODE analysis, demonstrates the activation of the core proteins NCF2, NCF4, CYBA and RAC1 by the shell proteins NCF1, PRKCZ and PARD6G. It is known that PRKCZ is activated by T cell receptor (Bertrand et al., 2010). In our analysis, it was observed that multiple T cell receptor signaling molecules were upregulated. We hypothesize that the TCR signaling via PRKCZ activates NCF complex which may subsequently generate ROS in the RA synovium. It is known that ROS can diffuse across

cell membranes to take part in intracellular signaling (Fisher, 2009). We believe that the activation of PRKCZ leading to the generation of ROS is one of the routes facilitating osteoclast differentiation in RA synovium. Our network also illustrated an upregulation of the catalytic subunit of PI3K, PIK3CD which is another downstream molecule of T cell receptor signaling. This is supported by the findings of Bartok et al (Bartok et al., 2012). PI3K-AKT pathway results in inhibition of the Forkhead box proteins, FOXO1 and FOXO3 (Patel & Mohan, 2005). It was shown that FOXO upregulates antioxidant enzymes that inhibit osteoclastogenesis (Bartell et al., 2014). In the ODP network, the downregulation of FOXO1 and FOXO3 is a possible indication of the presence of ROS mediated osteoclastogenesis in RA synovium. Bartell *et al* (Bartell et al., 2014), experimentally proved the role of RANKL in the downregulation of the Forkhead box proteins. In accordance with this, our analysis showed an upregulation of RANKL in the ODP network. Finally, our analysis reported the upregulation of the cytokine receptor CSF1R which is also required for osteoclastogenesis via PI3K-AKT pathway. The proposed model consisting of all the signaling routes promoting osteoclastogenesis via generation of ROS in the RA synovium is summarized in Fig. 10.

Conclusion

In this study, we have created a PPI network for osteoclast differentiation in the RA synovium for the first time using gene expression under RA conditions from microarray experiments, pathway enrichment analysis and protein protein interaction data. This network captures all the signaling routes that lead to osteoclastogenesis in the synovium and depicts the roles of T cell receptor signaling, canonical NF-κB pathway and ROS generation.

Data Availability: All the data generated and used for the analysis are included in this manuscript and in the Supplementary information. Abbreviations used are included in Table S11.

Abbreviations

ACP5	Acid Phosphatase 5, Tartrate Resistant (Tartrate-Resistant Acid Phosphatase – TRAP)
AKT	Akt Serine/Threonine Kinase 1 (protein Kinase B)
AMPK	5' Adenosine Monophosphate-Activated Protein Kinase
AP1	Activator Protein 1
BCL10	B Cell Cll/Lymphoma 10
BIRC2	Baculoviral Iap Repeat-Containing Protein 2 (Cellular Inhibitor Of Apoptosis 1)
BIRC3	Baculoviral Iap Repeat-Containing Protein 3 (Cellular Inhibitor Of Apoptosis 2)
CARD11	Caspase Recruitment Domain Family Member 11
CASP1	Caspase 1
CD247	T-Cell Surface Glycoprotein CD3 Zeta Chain
CD27	T-Cell Activation Antigen CD27
CD28	T-Cell-Specific Surface Glycoprotein Cd28
CD3E	T-Cell Surface Glycoprotein CD3 Epsilon Chain

608	CD47	Leukocyte Surface Antigen CD47 (integrin Associated Protein)
609	cGMP	Cyclic Guanosine Monophosphate
610	CRP	C-Reactive Protein
611	CSF1R	Colony Stimulating Factor 1 Receptor
612	CSK	C-Terminal Src Kinase
613	CTSK	Cathepsin K
614	CYBA	Cytochrome B-245 Alpha Chain
615	DAVID	Database for Annotation, Visualization and Integrated Discovery
616	DEG	Differentially expressed gene
617	EASE	Expression Analysis Systematic Explorer
618	ECM	Extra cellular matrix
619	ESR	Erythrocyte Sedimentation Rate
620	FAS	Fas cell Surface Death Receptor (CD95)
621	FCER1G	High Affinity Immunoglobulin Epsilon Receptor Subunit Gamma 3
622	FOS	Fos proto-oncogene
623	FOSB	Fosb Proto-Oncogene, Ap-1 Transcription Factor Subunit
624	FOXO1	Forkhead Box Protein O1
625	FOXO3	Forkhead Box Protein O3

626	FYB	Fyn Binding Protein
627	FZD4	Frizzled Class Receptor 4
628	GEO	Gene Expression Omnibus
629	GF	Growth Factor
630	GO	Gene Ontology
631	GOBP	Gene Ontology Biological Process
632	GOMF	Gene Ontology Molecular Function
633	GRN	Gene Regulatory Network
634	ID	Identifier
635	IFNAR2	Interferon Alpha And Beta Receptor Subunit 2
636	IFNβ	Interferon Beta
637	IgE	Immunoglobulin E
638	IGKC	Immunoglobulin Kappa Constant Region
639	IKK	Inhibitor Of Nuclear Factor Kappa B Kinase
640	IL1A	Interleukin 1 Alpha (hematopoietin 1)
641	IL1A	Interleukin 1 Alpha
642	IL1R1	Interleukin 1 Receptor Type 1
643	IL1RN	Interleukin 1 Receptor Antagonist

IL7R	Interleukin 7 Receptor
INPP5D	Inositol Polyphosphate-5-Phosphatase D
IκB	Nf-Kappa-B Inhibitor
IRAK4	Interleukin 1 Receptor Associated Kinase 4
ITK	Il2 Inducible T Cell Kinase
JAK2	Janus Kinase 2
JUN	Jun proto-Oncogene, Ap-1 Transcription Factor Subunit
JUNB	Junb Proto-Oncogene, Ap-1 Transcription Factor Subunit
KEGG	Kyoto Encyclopedia Of Genes And Genomes
LAT	Linker For Activation Of T Cells
LCK	Lymphocyte-Specific Protein Tyrosine Kinase
LCP2	Lymphocyte Cytosolic Protein 2 (Sh2 Domain Containing Leukocyte Protein Of 76kda)
LRP6	Ldl Receptor Related Protein 6
LYN	Lck/Yes-Related Novel Protein Tyrosine Kinase
MAP3K7	Mitogen-Activated Protein Kinase Kinase Kinase 7 (TGF-Beta Activated Kinase 1)
MAPK1	Mitogen-Activated Protein Kinase 1
MAS5	Microarray Suite 5.0

MYD88	Myeloid Differentiation Primary Response 88
NCF	Neutrophil Cytosol Factor
NCF1	Neutrophil Cytosolic Factor 1
NCF2	Neutrophil Cytosol Factor 2
NCF4	Neutrophil Cytosol Factor 4
NF-κB	Nuclear Factor Kappa-Light-Chain-Enhancer Of Activated B Cells
NFKBIA	Nf-κb Inhibitor Alpha
NFKBIB	Nf-κb Inhibitor Beta
NOD2	Nucleotide Binding Oligomerization Domain Containing Protein 2
Nox2	NADPH Oxidase 2
ODP	Osteoclast Differentiation Pathway
PAG1	Phosphoprotein Associated with Glycosphingolipid-enriched microdomains 1
PARD6G	Par-6 Family Cell Polarity Regulator Gamma
PELI1	Pellino E3 Ubiquitin Protein Ligase 1
PI3K	Phosphatidylinositol-4,5-Bisphosphate 3-Kinase
PIK3CD	Phosphatidylinositol-4,5-Bisphosphate 3-Kinase Catalytic Subunit Delta
PIK3CD	Phosphatidylinositol-4,5-Bisphosphate 3-Kinase Catalytic Subunit Delta
PKG	cGMP Dependent Protein Kinase (protein Kinase G)

682	PLCG2	Phospholipase C Gamma 2
683	PPARG	Peroxisome Proliferator Activated Receptor Gamma
684	PPI	Protein-Protein Interaction
685	PPIA	Peptidylprolyl Isomerase A (cyclophilin A)
686	PPP3CA	Protein Phosphatase 3 Catalytic Subunit Alpha (calcineurin A Alpha)
687	PPP3R1	Protein Phosphatase 3 Regulatory Subunit B, Alpha (calcineurin Subunit
688	B Type 1)	
689	PRKCB	Protein Kinase C Beta
690	PRKCQ	Protein Kinase C Theta
691	PRKCZ	Protein Kinase C Zeta
692	PTM	Post Translational Modification
693	RA	Rheumatoid Arthritis
694	RAC1	Rac Family Small GTPase 1
695	RANKL	Receptor Activator Of Nuclear Factor Kappa B Ligand
696	RCAN1	Regulator Of Calcineurin 1
697	REL	Rel proto-Oncogene, Nf-κb Subunit
698	RMA	Robust Multiarray Average
699	ROS	Reactive Oxygen Species
700	RPS6KA1	Ribosomal Protein S6 Kinase A1

701	RTK	Receptor Tyrosine Kinase
702	S100A13	S100 Calcium-Binding Protein A13
703	SFRP1	Secreted Frizzled Related Protein 1
704	SFRP2	Secreted Frizzled Related Protein 2
705	SFRP4	Secreted Frizzled Related Protein 4
706	SIRPA	Signal Regulatory Protein Alpha
707	SMAD3	Mothers Against Decapentaplegic Homolog 3
708	STAT1	Signal Transducer And Activator Of Transcription 1
709	STAT2	Signal Transducer And Activator Of Transcription 2
710	STRING	Search Tool For The Retrieval Of Interacting Genes/Proteins
711	TCR	T Cell Receptor
712	TF	Transcription Factor
713	TGFB1	Transforming Growth Factor Beta-1
714	TGFB2	Transforming Growth Factor Beta-2
715	TGFB3	Transforming Growth Factor Beta-3
716	TGFBR1	Tgf-Beta Receptor Type-1
717	TGFBR2	Tgf-Beta Receptor Type-2
718	TGFBR3	Tgf-Beta Receptor Type-3

719	TGFβ	Transforming Growth Factor Beta
720	TLR	Toll Like Receptor
721	TLR3	Toll Like Receptor 3
722	TLR4	Toll Like Receptor 4
723	TNFRSF11B	Tnf Receptor Superfamily Member 11b (Osteoprotegerin)
724	TNFRSF1A	Tumor Necrosis Factor Receptor 1
725	TNFSF11	Tumor Necrosis Factor Superfamily Member 11 (RANKL)
726	TRAF2	TNF Receptor Associated Factor 2
727	TRAF6	TNF Receptor Associated Factor 6
728	UBC	Ubiquitin C
729	XIAP	X-Linked Inhibitor Of Apoptosis
730	ZAP70	Zeta Chain Associated Protein Kinase 70

731 References

732 Assenov Y., Ramirez F., Schelhorn S-E., Lengauer T., Albrecht M. 2008. Computing topological
733 parameters of biological networks. *Bioinformatics (Oxford, England)* 24:282–284. DOI:
734 10.1093/bioinformatics/btm554.
735 Bader GD., Hogue CWV. 2003. An automated method for finding molecular complexes in large protein
736 interaction networks. *BMC bioinformatics* 4:2.

737 Bartell SM., Kim H-N., Ambrogini E., Han L., Iyer S., Serra Ucer S., Rabinovitch P., Jilka RL., Weinstein RS.,
738 Zhao H., O'Brien CA., Manolagas SC., Almeida M. 2014. FoxO proteins restrain
739 osteoclastogenesis and bone resorption by attenuating H2O2 accumulation. *Nature*
740 *communications* 5:3773. DOI: 10.1038/ncomms4773.
741 Bartok B., Boyle DL., Liu Y., Ren P., Ball ST., Bugbee WD., Rommel C., Firestein GS. 2012. PI3 kinase delta
742 is a key regulator of synoviocyte function in rheumatoid arthritis. *The American journal of*
743 *pathology* 180:1906–1916. DOI: 10.1016/j.ajpath.2012.01.030.
744 Bertrand F., Esquerre M., Petit A-E., Rodrigues M., Duchez S., Delon J., Valitutti S. 2010. Activation of the
745 ancestral polarity regulator protein kinase C zeta at the immunological synapse drives
746 polarization of Th cell secretory machinery toward APCs. *Journal of immunology (Baltimore,*
747 *Md. : 1950)* 185:2887–2894. DOI: 10.4049/jimmunol.1000739.
748 Broeren MGA., de Vries M., Bennink MB., Arntz OJ., Blom AB., Koenders MI., van Lent PLEM., van der
749 Kraan PM., van den Berg WB., van de Loo FAJ. 2016. Disease-Regulated Gene Therapy with Anti-
750 Inflammatory Interleukin-10 Under the Control of the CXCL10 Promoter for the Treatment of
751 Rheumatoid Arthritis. *Human gene therapy* 27:244–254. DOI: 10.1089/hum.2015.127.
752 Browner NC., Sellak H., Lincoln TM. 2004. Downregulation of cGMP-dependent protein kinase
753 expression by inflammatory cytokines in vascular smooth muscle cells. *American journal of*
754 *physiology. Cell physiology* 287:C88-96. DOI: 10.1152/ajpcell.00039.2004.
755 Chang M., Jin W., Chang J-H., Xiao Y., Brittain G., Yu J., Zhou X., Wang Y-H., Cheng X., Li P., Rabinovich
756 BA., Hwu P., Sun S-C. 2011. Peli1 negatively regulates T-cell activation and prevents
757 autoimmunity. *Nature immunology* 12:1002–1009. DOI: 10.1038/ni.2090.
758 Davis S., Meltzer PS. 2007. GEOquery: a bridge between the Gene Expression Omnibus (GEO) and
759 BioConductor. *Bioinformatics (Oxford, England)* 23:1846–1847. DOI:
760 10.1093/bioinformatics/btm254.

761 Dey P., Panga V., Raghunathan S. 2016. A Cytokine Signalling Network for the Regulation of Inducible
762 Nitric Oxide Synthase Expression in Rheumatoid Arthritis. *PloS one* 11:e0161306. DOI:
763 10.1371/journal.pone.0161306.
764 Dooley S., Herlitzka I., Hanselmann R., Ermis A., Henn W., Remberger K., Hopf T., Welter C. 1996.
765 Constitutive expression of c-fos and c-jun, overexpression of ets-2, and reduced expression of
766 metastasis suppressor gene nm23-H1 in rheumatoid arthritis. *Annals of the rheumatic diseases*
767 55:298–304.
768 Edgar R., Domrachev M., Lash AE. 2002. Gene Expression Omnibus: NCBI gene expression and
769 hybridization array data repository. *Nucleic acids research* 30:207–210.
770 Expansion of the Gene Ontology knowledgebase and resources. 2017. *Nucleic acids research* 45:D331–
771 D338. DOI: 10.1093/nar/gkw1108.
772 Fionda C., Nappi F., Piccoli M., Frati L., Santoni A., Cippitelli M. 2007. 15-Deoxy-$\Delta^{12,14}$-Prostaglandin J_2
773 Negatively Regulates rankl Gene Expression in Activated T Lymphocytes: Role of NF-
774 κB and Early Growth Response Transcription Factors. *The Journal of Immunology* 178:4039. DOI:
775 10.4049/jimmunol.178.7.4039.
776 Fisher AB. 2009. Redox Signaling Across Cell Membranes. *Antioxidants & Redox Signaling* 11:1349–1356.
777 DOI: 10.1089/ars.2008.2378.
778 Franca R., Vieira SM., Talbot J., Peres RS., Pinto LG., Zamboni DS., Louzada-Junior P., Cunha FQ., Cunha
779 TM. 2016. Expression and activity of NOD1 and NOD2/RIPK2 signalling in mononuclear cells
780 from patients with rheumatoid arthritis. *Scandinavian journal of rheumatology* 45:8–12. DOI:
781 10.3109/03009742.2015.1047403.
782 Gautier L., Cope L., Bolstad BM., Irizarry RA. 2004. affy--analysis of Affymetrix GeneChip data at the
783 probe level. *Bioinformatics (Oxford, England)* 20:307–315. DOI: 10.1093/bioinformatics/btg405.

784 Gloire G., Legrand-Poels S., Piette J. 2006. NF-kappaB activation by reactive oxygen species: fifteen years
785 later. *Biochemical pharmacology* 72:1493–1505. DOI: 10.1016/j.bcp.2006.04.011.
786 Grabiec AM., Angiolilli C., Hartkamp LM., van Baarsen LGM., Tak PP., Reedquist KA. 2015. JNK-
787 dependent downregulation of FoxO1 is required to promote the survival of fibroblast-like
788 synoviocytes in rheumatoid arthritis. *Annals of the rheumatic diseases* 74:1763–1771. DOI:
789 10.1136/annrheumdis-2013-203610.
790 Gravallese EM., Harada Y., Wang JT., Gorn AH., Thornhill TS., Goldring SR. 1998. Identification of cell
791 types responsible for bone resorption in rheumatoid arthritis and juvenile rheumatoid arthritis.
792 *The American journal of pathology* 152:943–951.
793 Grigoriadis AE., Wang ZQ., Cecchini MG., Hofstetter W., Felix R., Fleisch HA., Wagner EF. 1994. c-Fos: a
794 key regulator of osteoclast-macrophage lineage determination and bone remodeling. *Science*
795 *(New York, N.Y.)* 266:443–448.
796 Gruber B., Ballan D., Gorevic PD. 1988. IgE rheumatoid factors: quantification in synovial fluid and ability
797 to induce synovial mast cell histamine release. *Clinical and Experimental Immunology* 71:289–
798 294.
799 Hao R., Du H., Guo L., Tian F., An N., Yang T., Wang C., Wang B., Zhou Z. 2017. Identification of
800 dysregulated genes in rheumatoid arthritis based on bioinformatics analysis. *PeerJ* 5:e3078. DOI:
801 10.7717/peerj.3078.
802 Hosack DA., Dennis G., Sherman BT., Lane HC., Lempicki RA. 2003. Identifying biological themes within
803 lists of genes with EASE. *Genome Biology* 4:P4. DOI: 10.1186/gb-2003-4-6-p4.
804 Huang DW., Sherman BT., Lempicki RA. 2009a. Systematic and integrative analysis of large gene lists
805 using DAVID bioinformatics resources. *Nature protocols* 4:44–57. DOI: 10.1038/nprot.2008.211.

806 Huang DW., Sherman BT., Lempicki RA. 2009b. Bioinformatics enrichment tools: paths toward the
807 comprehensive functional analysis of large gene lists. *Nucleic acids research* 37:1–13. DOI:
808 10.1093/nar/gkn923.
809 Huber R., Hummert C., Gausmann U., Pohlers D., Koczan D., Guthke R., Kinne RW. 2008. Identification of
810 intra-group, inter-individual, and gene-specific variances in mRNA expression profiles in the
811 rheumatoid arthritis synovial membrane. *Arthritis research & therapy* 10:R98. DOI:
812 10.1186/ar2485.
813 Jeong H., Baek SY., Kim SW., Eun YH., Kim IY., Kim H., Lee J., Koh E-M., Cha H-S. 2017. Comorbidities of
814 rheumatoid arthritis: Results from the Korean National Health and Nutrition Examination
815 Survey. *PloS one* 12:e0176260. DOI: 10.1371/journal.pone.0176260.
816 Jung SM., Kim KW., Yang C-W., Park S-H., Ju JH. 2014. Cytokine-Mediated Bone Destruction in
817 Rheumatoid Arthritis. *Journal of Immunology Research* 2014. DOI: 10.1155/2014/263625.
818 Kanehisa M., Furumichi M., Tanabe M., Sato Y., Morishima K. 2017. KEGG: new perspectives on
819 genomes, pathways, diseases and drugs. *Nucleic acids research* 45:D353–D361. DOI:
820 10.1093/nar/gkw1092.
821 Kang IS., Kim C. 2016. NADPH oxidase gp91(phox) contributes to RANKL-induced osteoclast
822 differentiation by upregulating NFATc1. *Scientific reports* 6:38014. DOI: 10.1038/srep38014.
823 Karst M., Gorny G., Galvin RJS., Oursler MJ. 2004. Roles of stromal cell RANKL, OPG, and M-CSF
824 expression in biphasic TGF-beta regulation of osteoclast differentiation. *Journal of cellular*
825 *physiology* 200:99–106. DOI: 10.1002/jcp.20036.
826 Kinne RW., Boehm S., Iftner T., Aigner T., Vornehm S., Weseloh G., Bravo R., Emmrich F., Kroczek RA.
827 1995. Synovial fibroblast-like cells strongly express jun-B and C-fos proto-oncogenes in
828 rheumatoid- and osteoarthritis. *Scandinavian journal of rheumatology. Supplement* 101:121–
829 125.

830 Kupfer P., Huber R., Weber M., Vlaic S., Haupl T., Koczan D., Guthke R., Kinne RW. 2014. Novel
831 application of multi-stimuli network inference to synovial fibroblasts of rheumatoid arthritis
832 patients. *BMC medical genomics* 7:40. DOI: 10.1186/1755-8794-7-40.
833 Lee H., Kashiwakura J., Matsuda A., Watanabe Y., Sakamoto-Sasaki T., Matsumoto K., Hashimoto N.,
834 Saito S., Ohmori K., Nagaoka M., Tokuhashi Y., Ra C., Okayama Y. 2013. Activation of human
835 synovial mast cells from rheumatoid arthritis or osteoarthritis patients in response to
836 aggregated IgG through Fcgamma receptor I and Fcgamma receptor II. *Arthritis and rheumatism*
837 65:109–119. DOI: 10.1002/art.37741.
838 Lee H-M., Sugino H., Aoki C., Shimaoka Y., Suzuki R., Ochi K., Ochi T., Nishimoto N. 2011. Abnormal
839 networks of immune response-related molecules in bone marrow cells from patients with
840 rheumatoid arthritis as revealed by DNA microarray analysis. *Arthritis research & therapy*
841 13:R89. DOI: 10.1186/ar3364.
842 Li X-F., Sun Y-Y., Bao J., Chen X., Li Y-H., Yang Y., Zhang L., Huang C., Wu B-M., Meng X-M., Li J. 2017.
843 Functional role of PPAR-gamma on the proliferation and migration of fibroblast-like
844 synoviocytes in rheumatoid arthritis. *Scientific reports* 7:12671. DOI: 10.1038/s41598-017-
845 12570-6.
846 Lories RJ., Corr M., Lane NE. 2013. To Wnt or not to Wnt: the bone and joint health dilemma. *Nature*
847 *reviews. Rheumatology* 9:328–339. DOI: 10.1038/nrrheum.2013.25.
848 Ludikhuize J., de Launay D., Groot D., Smeets TJM., Vinkenoog M., Sanders ME., Tas SW., Tak PP.,
849 Reedquist KA. 2007. Inhibition of forkhead box class O family member transcription factors in
850 rheumatoid synovial tissue. *Arthritis and rheumatism* 56:2180–2191. DOI: 10.1002/art.22653.
851 Lutzny G., Kocher T., Schmidt-Supprian M., Rudelius M., Klein-Hitpass L., Finch AJ., Dürig J., Wagner M.,
852 Haferlach C., Kohlmann A., Schnittger S., Seifert M., Wanninger S., Zaborsky N., Oostendorp R.,
853 Ruland J., Leitges M., Kuhnt T., Schäfer Y., Lampl B., Peschel C., Egle A., Ringshausen I. 2013.

Protein Kinase C-β-Dependent Activation of NF-κB in Stromal Cells Is Indispensable for the Survival of Chronic Lymphocytic Leukemia B Cells In Vivo. *Cancer Cell* 23:77–92. DOI: 10.1016/j.ccr.2012.12.003.

McInnes IB., Schett G. 2007. Cytokines in the pathogenesis of rheumatoid arthritis. *Nature reviews. Immunology* 7:429–442. DOI: 10.1038/nri2094.

McInnes IB., Schett G. 2011. The pathogenesis of rheumatoid arthritis. *The New England journal of medicine* 365:2205–2219. DOI: 10.1056/NEJMra1004965.

Miao C., Yang Y., He X., Li X., Huang C., Huang Y., Zhang L., Lv X-W., Jin Y., Li J. 2013. Wnt signaling pathway in rheumatoid arthritis, with special emphasis on the different roles in synovial inflammation and bone remodeling. *Cellular signalling* 25:2069–2078. DOI: 10.1016/j.cellsig.2013.04.002.

Nevius E., Gomes AC., Pereira JP. 2016. A comprehensive review of inflammatory cell migration in rheumatoid arthritis. *Clinical reviews in allergy & immunology* 51:59–78. DOI: 10.1007/s12016-015-8520-9.

Otterness IG. 1994. The value of C-reactive protein measurement in rheumatoid arthritis. *Seminars in arthritis and rheumatism* 24:91–104.

Patel RK., Mohan C. 2005. PI3K/AKT signaling and systemic autoimmunity. *Immunologic research* 31:47–55. DOI: 10.1385/IR:31:1:47.

Pepper SD., Saunders EK., Edwards LE., Wilson CL., Miller CJ. 2007. The utility of MAS5 expression summary and detection call algorithms. *BMC Bioinformatics* 8:273. DOI: 10.1186/1471-2105-8-273.

R Core Team. 2017. R: A language and environment for statistical computing. R Foundation for Statistical Computing, Vienna, Austria. URL https://www.R-project.org/.

877 Raker VK., Becker C., Steinbrink K. 2016. The cAMP Pathway as Therapeutic Target in Autoimmune and
878 Inflammatory Diseases. *Frontiers in Immunology* 7. DOI: 10.3389/fimmu.2016.00123.
879 Rosen GM., Pou S., Ramos CL., Cohen MS., Britigan BE. 1995. Free radicals and phagocytic cells. *FASEB*
880 *journal : official publication of the Federation of American Societies for Experimental Biology*
881 9:200–209.
882 Sams M., Olsen MA., Joshi R., Ranganathan P. 2015. Staphylococcus aureus sepsis in rheumatoid
883 arthritis. *Rheumatology international* 35:1503–1510. DOI: 10.1007/s00296-015-3239-8.
884 Schett G. 2007. Cells of the synovium in rheumatoid arthritis. Osteoclasts. *Arthritis research & therapy*
885 9:203. DOI: 10.1186/ar2110.
886 Shannon P., Markiel A., Ozier O., Baliga NS., Wang JT., Ramage D., Amin N., Schwikowski B., Ideker T.
887 2003. Cytoscape: a software environment for integrated models of biomolecular interaction
888 networks. *Genome research* 13:2498–2504. DOI: 10.1101/gr.1239303.
889 Shih VF-S., Tsui R., Caldwell A., Hoffmann A. 2011. A single NFκB system for both canonical and non-
890 canonical signaling. *Cell Research* 21:86–102. DOI: 10.1038/cr.2010.161.
891 Sommer K., Guo B., Pomerantz JL., Bandaranayake AD., Moreno-Garcia ME., Ovechkina YL., Rawlings DJ.
892 2005. Phosphorylation of the CARMA1 linker controls NF-kappaB activation. *Immunity* 23:561–
893 574. DOI: 10.1016/j.immuni.2005.09.014.
894 Speirs C., Williams JJL., Riches K., Salt IP., Palmer TM. 2018. Linking energy sensing to suppression of JAK-
895 STAT signalling: A potential route for repurposing AMPK activators? *Pharmacological research*
896 128:88–100. DOI: 10.1016/j.phrs.2017.10.001.
897 Szamel M., Bartels F., Resch K. 1993. Cyclosporin A inhibits T cell receptor-induced interleukin-2
898 synthesis of human T lymphocytes by selectively preventing a transmembrane signal
899 transduction pathway leading to sustained activation of a protein kinase C isoenzyme, protein
900 kinase. *European journal of immunology* 23:3072–3081. DOI: 10.1002/eji.1830231205.

Szklarczyk D., Franceschini A., Wyder S., Forslund K., Heller D., Huerta-Cepas J., Simonovic M., Roth A., Santos A., Tsafou KP., Kuhn M., Bork P., Jensen LJ., von Mering C. 2015. STRING v10: protein-protein interaction networks, integrated over the tree of life. *Nucleic acids research* 43:D447-452. DOI: 10.1093/nar/gku1003.

Tak PP., Hintzen RQ., Teunissen JJ., Smeets TJ., Daha MR., van Lier RA., Kluin PM., Meinders AE., Swaak AJ., Breedveld FC. 1996. Expression of the activation antigen CD27 in rheumatoid arthritis. *Clinical immunology and immunopathology* 80:129–138.

Tenenbaum D. 2017. KEGGREST: Client-side REST access to KEGG. R package version 1.14.1.

Tetlow LC., Woolley DE. 1995. Mast cells, cytokines, and metalloproteinases at the rheumatoid lesion: dual immunolocalisation studies. *Annals of the rheumatic diseases* 54:896–903.

Turvey SE., Durandy A., Fischer A., Fung S-Y., Geha RS., Gewies A., Giese T., Greil J., Keller B., McKinnon ML., Neven B., Rozmus J., Ruland J., Snow AL., Stepensky P., Warnatz K. 2014. The CARD11-BCL10-MALT1 (CBM) signalosome complex: Stepping into the limelight of human primary immunodeficiency. *The Journal of allergy and clinical immunology* 134:276–284. DOI: 10.1016/j.jaci.2014.06.015.

Ungethuem U., Haeupl T., Witt H., Koczan D., Krenn V., Huber H., von Helversen TM., Drungowski M., Seyfert C., Zacher J., Pruss A., Neidel J., Lehrach H., Thiesen HJ., Ruiz P., Blass S. 2010. Molecular signatures and new candidates to target the pathogenesis of rheumatoid arthritis. *Physiological genomics* 42A:267–282. DOI: 10.1152/physiolgenomics.00004.2010.

Varfolomeev E., Blankenship JW., Wayson SM., Fedorova AV., Kayagaki N., Garg P., Zobel K., Dynek JN., Elliott LO., Wallweber HJA., Flygare JA., Fairbrother WJ., Deshayes K., Dixit VM., Vucic D. 2007. IAP antagonists induce autoubiquitination of c-IAPs, NF-kappaB activation, and TNFalpha-dependent apoptosis. *Cell* 131:669–681. DOI: 10.1016/j.cell.2007.10.030.

924 Vasudevan D., Ryoo HD. 2015. Regulation of Cell Death by IAPs and Their Antagonists. *Current topics in*
925 *developmental biology* 114:185–208. DOI: 10.1016/bs.ctdb.2015.07.026.
926 Wang H., Guo J., Jiang J., Wu W., Chang X., Zhou H., Li Z., Zhao J. 2017. New genes associated with
927 rheumatoid arthritis identified by gene expression profiling. *International journal of*
928 *immunogenetics* 44:107–113. DOI: 10.1111/iji.12313.
929 Wang P., Heitman J. 2005. The cyclophilins. *Genome Biology* 6:226. DOI: 10.1186/gb-2005-6-7-226.
930 Wetteland P., Roger M., Solberg HE., Iversen OH. 1996. Population-based erythrocyte sedimentation
931 rates in 3910 subjectively healthy Norwegian adults. A statistical study based on men and
932 women from the Oslo area. *Journal of internal medicine* 240:125–131.
933 Wilson CL., Miller CJ. 2005. Simpleaffy: a BioConductor package for Affymetrix Quality Control and data
934 analysis. *Bioinformatics (Oxford, England)* 21:3683–3685. DOI: 10.1093/bioinformatics/bti605.
935 Wishart DS., Feunang YD., Guo AC., Lo EJ., Marcu A., Grant JR., Sajed T., Johnson D., Li C., Sayeeda Z.,
936 Assempour N., Iynkkaran I., Liu Y., Maciejewski A., Gale N., Wilson A., Chin L., Cummings R., Le
937 D., Pon A., Knox C., Wilson M. 2018. DrugBank 5.0: a major update to the DrugBank database for
938 2018. *Nucleic acids research* 46:D1074–D1082. DOI: 10.1093/nar/gkx1037.
939 Woetzel D., Huber R., Kupfer P., Pohlers D., Pfaff M., Driesch D., Haupl T., Koczan D., Stiehl P., Guthke R.,
940 Kinne RW. 2014. Identification of rheumatoid arthritis and osteoarthritis patients by
941 transcriptome-based rule set generation. *Arthritis research & therapy* 16:R84. DOI:
942 10.1186/ar4526.
943 Wu G., Zhu L., Dent JE., Nardini C. 2010. A comprehensive molecular interaction map for rheumatoid
944 arthritis. *PloS one* 5:e10137. DOI: 10.1371/journal.pone.0010137.
945 Xiong Q., Zhang L., Ge W., Tang P. 2016. The roles of interferons in osteoclasts and osteoclastogenesis.
946 *Joint, bone, spine : revue du rhumatisme* 83:276–281. DOI: 10.1016/j.jbspin.2015.07.010.

947 You S., Yoo S-A., Choi S., Kim J-Y., Park S-J., Ji JD., Kim T-H., Kim K-J., Cho C-S., Hwang D., Kim W-U. 2014.
948 Identification of key regulators for the migration and invasion of rheumatoid synoviocytes
949 through a systems approach. *Proceedings of the National Academy of Sciences of the United*
950 *States of America* 111:550–555. DOI: 10.1073/pnas.1311239111.
951 Zhu Y., Davis S., Stephens R., Meltzer PS., Chen Y. 2008. GEOmetadb: powerful alternative search engine
952 for the Gene Expression Omnibus. *Bioinformatics (Oxford, England)* 24:2798–2800. DOI:
953 10.1093/bioinformatics/btn520.
954

Table 1(on next page)

The details of the databases used in this study.

The name and the reference of the database is listed in the column named “Database”. The type of data used from the database and the features of the database are described in the table. The rationale for using the data from each of the databases in our study is included in the table.

1

Database	Type of data obtained for this study	Features	Rationale
GEO (Edgar, Domrachev & Lash, 2002)	microarray gene expression data	GEO is a public repository with easy access to high throughput data, including microarray data and related metadata such as tissue type, disease state etc.	Microarray data from GEO database was used to identify DEGs in the RA synovium
DAVID - Gene ID conversion tool (Huang, Sherman & Lempicki, 2009b) (Huang, Sherman & Lempicki, 2009a)	Gene ID types	The DAVID knowledge base supports conversion between more than 20 gene ID types, including Affymetrix probe IDs.	The DAVID gene ID conversion table was used to convert Affymetrix probe IDs to Entrez IDs.
KEGG pathway (Kanehisa et al., 2017)	molecular pathways	KEGG pathways are manually drawn and frequently updated. References are provided for each pathway.	The KEGG pathway database was used to identify the enriched pathways from the list of DEGs.
String (v10) (Szklarczyk et al., 2015)	protein-protein interaction	String integrates information from several sources including experimental results from literature, and provides a confidence score for the interaction.	The String database was used to identify the proteins that directly interacted with KEGG osteoclast differentiation pathway proteins. These proteins (KEGG osteoclast differentiation pathway proteins and their interactors) were used to create a PPI network for osteoclast differentiation.
Gene Ontology ("Expansion of the Gene Ontology knowledgebase and	functional annotation	Gene Ontology annotation associates genes to specific functional terms. A	GO enrichment was used to identify the functions associated with the proteins in the osteoclast

resources.," 2017)		GO enrichment analysis provides information about functions that a set of genes may be involved in.	differentiation PPI network.
DrugBank (Wishart et al., 2018)	drug targets	DrugBank provides comprehensive information of drug targets and drug types (small molecule, biologics *etc*.)	DrugBank was used to identify proteins in the network that are targets of RA drugs.

2

Table 2(on next page)

The details of the microarray datasets from GEO repository used in our study

The accession number and the reference of the datasets is listed in the column named “Accession Number”. The title of the Affymetrix platform used by the particular dataset in included in the “Platform” column of the table. The information on the number of the RA patients and healthy controls used in each dataset are included in this table. Gender distribution is provided for the datasets GSE12021(U133A) and 12021 (U133B).

Accession Number	Platform	Rheumatoid arthritis samples	Healthy control samples
GSE1919(Ungethuem et al., 2010)	Affymetrix Human Genome U95A Array	5	5
GSE7307	Affymetrix Human Genome U133 Plus 2.0 Array	5	9
GSE12021(Huber et al., 2008)	Affymetrix Human Genome U133A Array	12 [3m/9f]	9 [7m/2f]
	Affymetrix Human Genome U133B Array	12 [3m/9f]	4 [3m/1f]
GSE55235(Woetzel et al., 2014)	Affymetrix Human Genome U133A Array	10	10
GSE55457(Woetzel et al., 2014)	Affymetrix Human Genome U133A Array	13	10
GSE77298(Broeren et al., 2016)	Affymetrix Human Genome U133 Plus 2.0 Array	16	7

1

Table 3(on next page)

Datasets showing downregulation of AP1 proteins in the RA synovium.

This table includes the information about the downregulation of the AP1 proteins as obtained by different microarray datasets used in our study.

Dataset	FOSB	JUN	JUNB
GSE1919	Downregulation	No differential regulation	No differential regulation
GSE7307	No differential regulation	Downregulation	No differential regulation
GSE12021 [U133A]	Downregulation	Downregulation	Downregulation
GSE55235	Downregulation	Downregulation	Downregulation
GSE55457	Downregulation	Downregulation	Downregulation

1

Table 4(on next page)

Upregulated signaling pathways in the RA synovium and their KEGG categories.

The numbers prefixed with “hsa” are the KEGG identifiers for each pathway. The KEGG pathway term name along with the KEGG pathway identifier is listed in the column named “Pathways”. The “Fold enrichment” is calculated based on the number of upregulated genes which belong to the KEGG pathway term (“Count”), total number of upregulated genes which are part of the KEGG pathway database (“List Total”), total number of genes that belong to the KEGG Pathway database (“Population Total”) and number of the KEGG Pathway database genes which are part of the KEGG pathway term (“Population Hits”). Precisely, the “Fold enrichment” is the proportion of “Count”/ “List Total” to “Population Hits”/ “Population Total” The “EASE score” represents the significance of obtaining “Count” genes in the “List Total” for the given KEGG pathway term which has “Population Hits” genes in the background “Population Total”.

Pathways	KEGG Categories	Fold enrichment	EASE score
hsa04064:NF-κB signaling pathway	Signal transduction	3.92	$6.25\ e^{-9}$
hsa04664:Fc-ε RI signaling pathway	Immune system	3.19	$8.96\ e^{-5}$
hsa04621:NOD-like receptor signaling pathway	Immune system	3.11	$6.68\ e^{-4}$
hsa04662:B cell receptor signaling pathway	Immune system	3.05	$1.53\ e^{-4}$
hsa04620:Toll-like receptor signaling pathway	Immune system	2.89	$1.35\ e^{-5}$
hsa04062:Chemokine signaling pathway	Immune system	2.82	$4.96\ e^{-9}$
hsa04660:T cell receptor signaling pathway	Immune system	2.30	$1.69\ e^{-3}$
hsa04630:JAK-STAT signaling pathway	Signal transduction	1.96	$4.45\ e^{-3}$

1

Table 5(on next page)

Downregulated signaling pathways in the RA synovium and their KEGG categories.

The numbers prefixed with “hsa” are the KEGG identifiers for each pathway. The KEGG pathway term name along with the KEGG pathway identifier is listed in the column named “Pathways”. The “Fold enrichment” is calculated based on the number of downregulated genes which belong to the KEGG pathway term (“Count”), total number of downregulated genes which are part of the KEGG pathway database (“List Total”), total number of genes that belong to the KEGG Pathway database (“Population Total”) and number of the KEGG Pathway database genes which are part of the KEGG pathway term (“Population Hits”). Precisely, the “Fold enrichment” is the proportion of “Count”/ “List Total” to “Population Hits”/ “Population Total” The “EASE score” represents the significance of obtaining “count” genes in the “List Total” for the given KEGG pathway term which has “Population Hits” genes in the background “Population Total”.

Pathways	KEGG Categories	Fold enrichment	EASE score
hsa04350:TGF-beta signaling pathway	Signal transduction	2.42	9.49 e^{-3}
hsa04152:AMPK signaling pathway	Signal transduction	2.30	2.56 e^{-3}
hsa04068:FoxO signaling pathway	Signal transduction	2.09	6.57 e^{-3}
hsa04022:cGMP-PKG signaling pathway	Signal transduction	1.90	9.85 e^{-3}
hsa04310:Wnt signaling pathway	Signal transduction	1.83	3.26 e^{-2}
hsa04024:cAMP signaling pathway	Signal transduction	1.62	4.37 e^{-2}
hsa04010:MAPK signaling pathway	Signal transduction	1.55	3.27 e^{-2}

1

Figure 1

The workflow.

(A). Selection of a KEGG pathway representing a phenotype exhibited by the RA synovium. The differentially expressed genes in the RA synovium were identified from the analysis of the microarray datasets obtained from GEO database. A KEGG pathway enrichment analysis was performed on the differentially expressed gene lists. The enriched pathways were categorized into process and signaling pathways. Based on the shared differentially expressed genes, a pathway overlap network was created. Osteoclast differentiation pathway was selected as the pathway of interest as it overlapped with most number of signaling pathways. **(B). Construction and analysis of the osteoclast differentiation network.** The proteins belonging to the KEGG osteoclast differentiation pathway were termed as “core proteins”. The core proteins were used as an input to the String DB to obtain the proteins interacting with them (first shell proteins). The interactions among all the proteins (core and first shell) were also extracted from String DB. The interactions were validated using PubMed. The directions of the protein interactions were also obtained. The proteins and the interactions were used to construct a network for osteoclast differentiation. The gene ontology term enrichment analysis was performed on the network. Differentially regulated genes were indicated in the network. The gene ontology term enrichment analysis and the differentially regulated genes were used to identify the important protein interactions that lead to osteoclast differentiation in the RA synovium. The protein targets of the drugs used in RA treatment were obtained from DrugBank database and were indicated in the network.

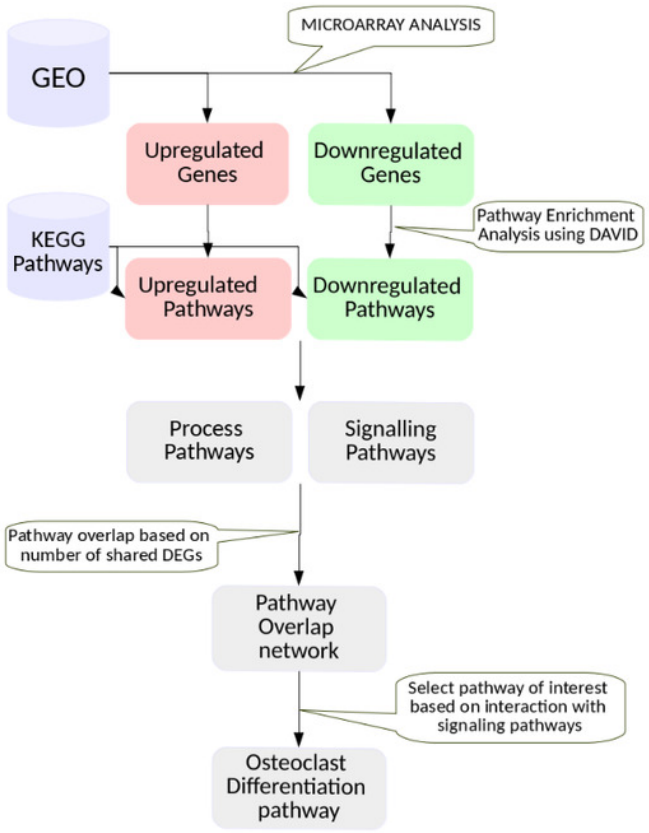
MICROARRAY ANALYSIS
GEO
Upregulated Genes
Downregulated Genes
Pathway Enrichment Analysis using DAVID
KEGG Pathways
Upregulated Pathways
Downregulated Pathways
Process Pathways
Signalling Pathways
Pathway overlap based on number of shared DEGs
Pathway Overlap network
Select pathway of interest based on interaction with signaling pathways
Osteoclast Differentiation pathway

A

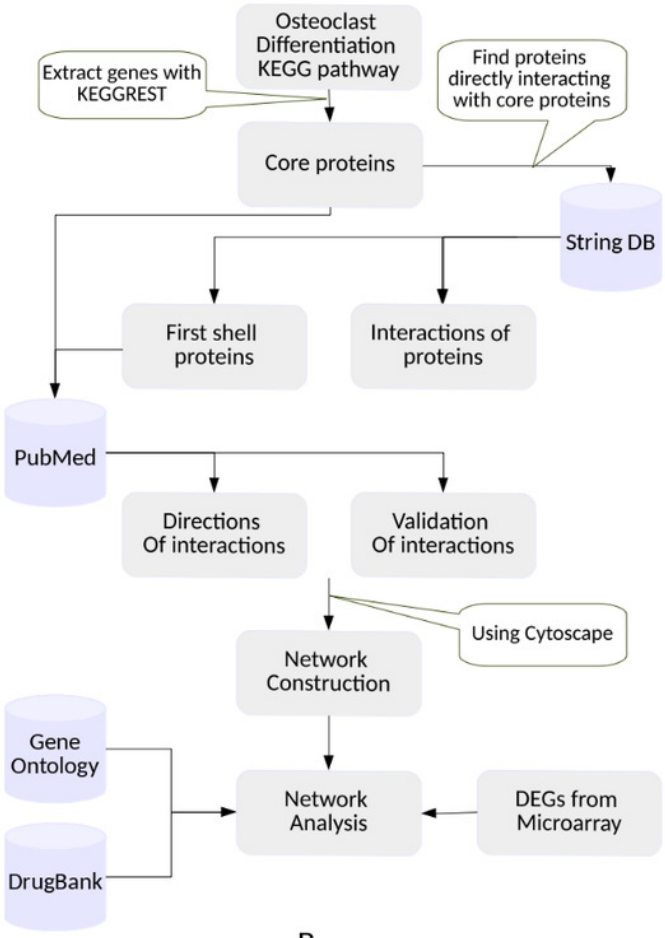
Osteoclast Differentiation KEGG pathway
Extract genes with KEGGREST
Find proteins directly interacting with core proteins
Core proteins
String DB
First shell proteins
Interactions of proteins
PubMed
Directions Of interactions
Validation Of interactions
Using Cytoscape
Network Construction
Gene Ontology
DrugBank
Network Analysis
DEGs from Microarray

B

Figure 2

Number of up and downregulated genes obtained based on the selection criteria.

The numbers on x-axis represent the following: “1”: selection of the genes at least once by the algorithm MAS5 and RMA, “2”: selection of the genes at least twice by both the algorithms, “3”: selection of the genes at least thrice by both the algorithms and so on. The y-axis represents the number of selected up and downregulated genes. The number of differentially expressed genes selected at least once by both the algorithms are used in this study.

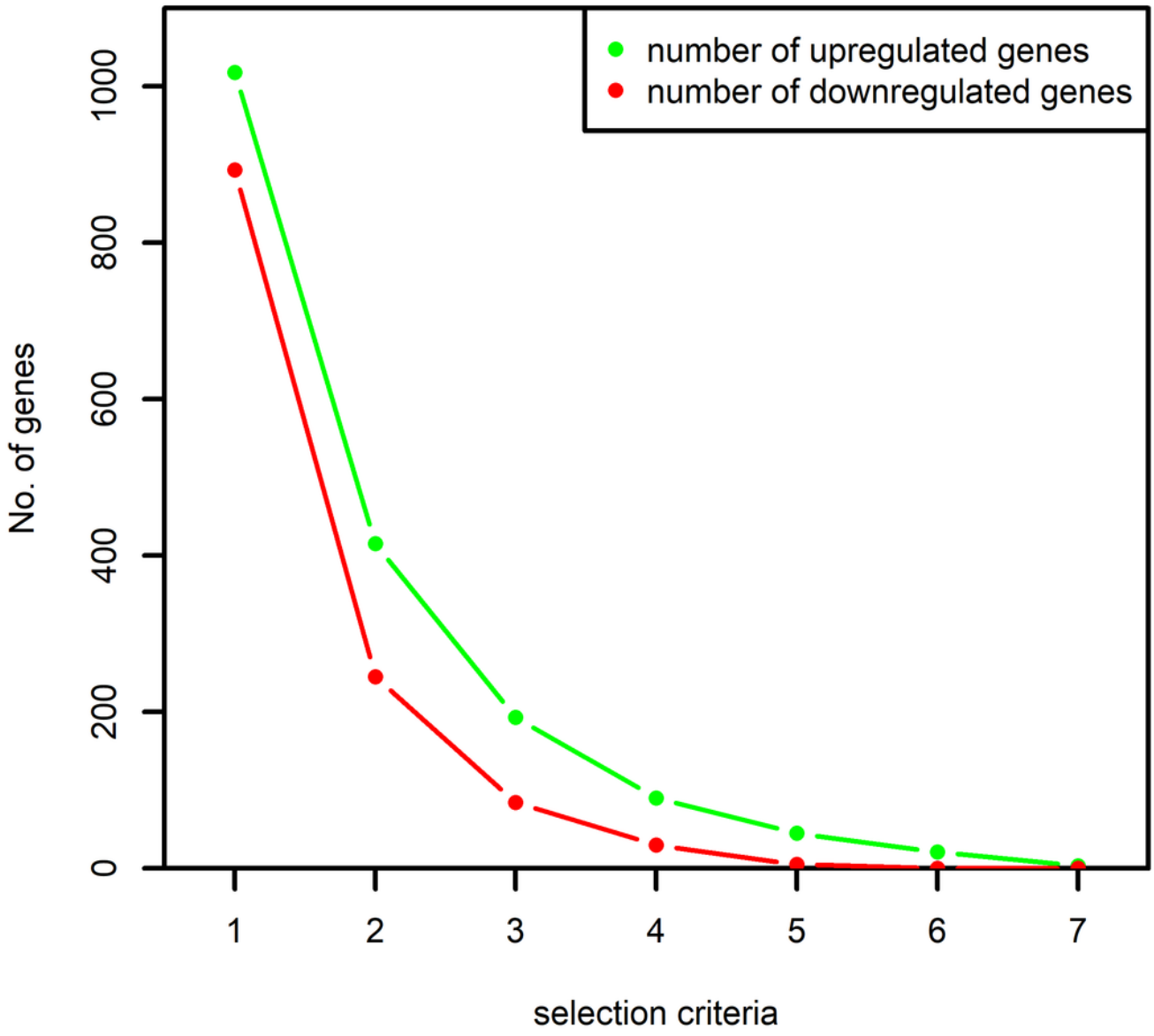
number of upregulated genes
number of downregulated genes
No. of genes
0
200
400
600
800
1000
1
2
3
4
5
6
7
selection criteria

Figure 3

Number of up and downregulated genes shared by pairs of pathways.

The numbers on x-axis represent the sum of all the genes belonging to the pathway pairs. The y-axis represents the number of up and downregulated genes common to the pairs. The pathway pairs sharing at least 5 up or 5 downregulated genes are used in this study.

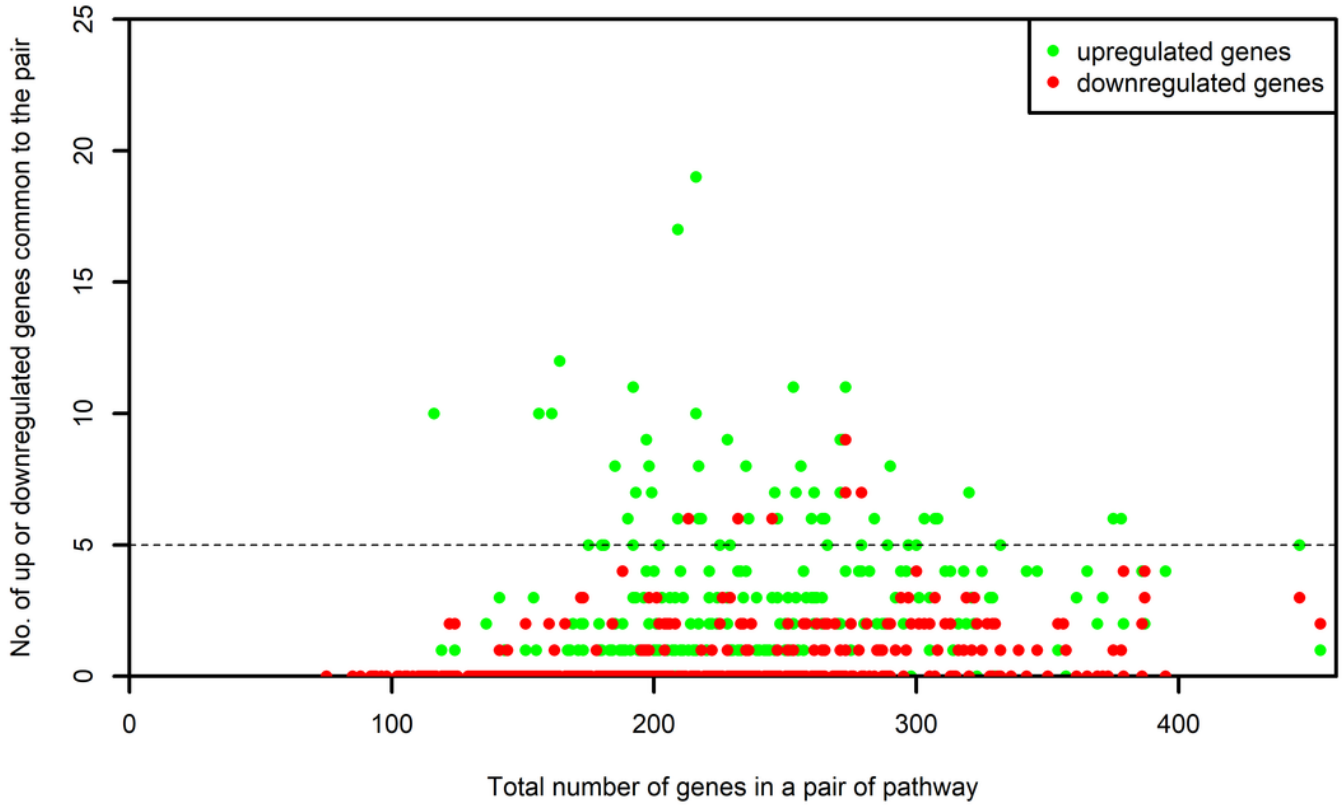

Figure 4

The KEGG category-wise distribution of the enriched pathways in the upregulated genes of the RA synovium.

The x-axis represents the KEGG categories as listed in the KEGG database whereas the y-axis denotes the number of enriched pathways from our study belonging to the KEGG categories.

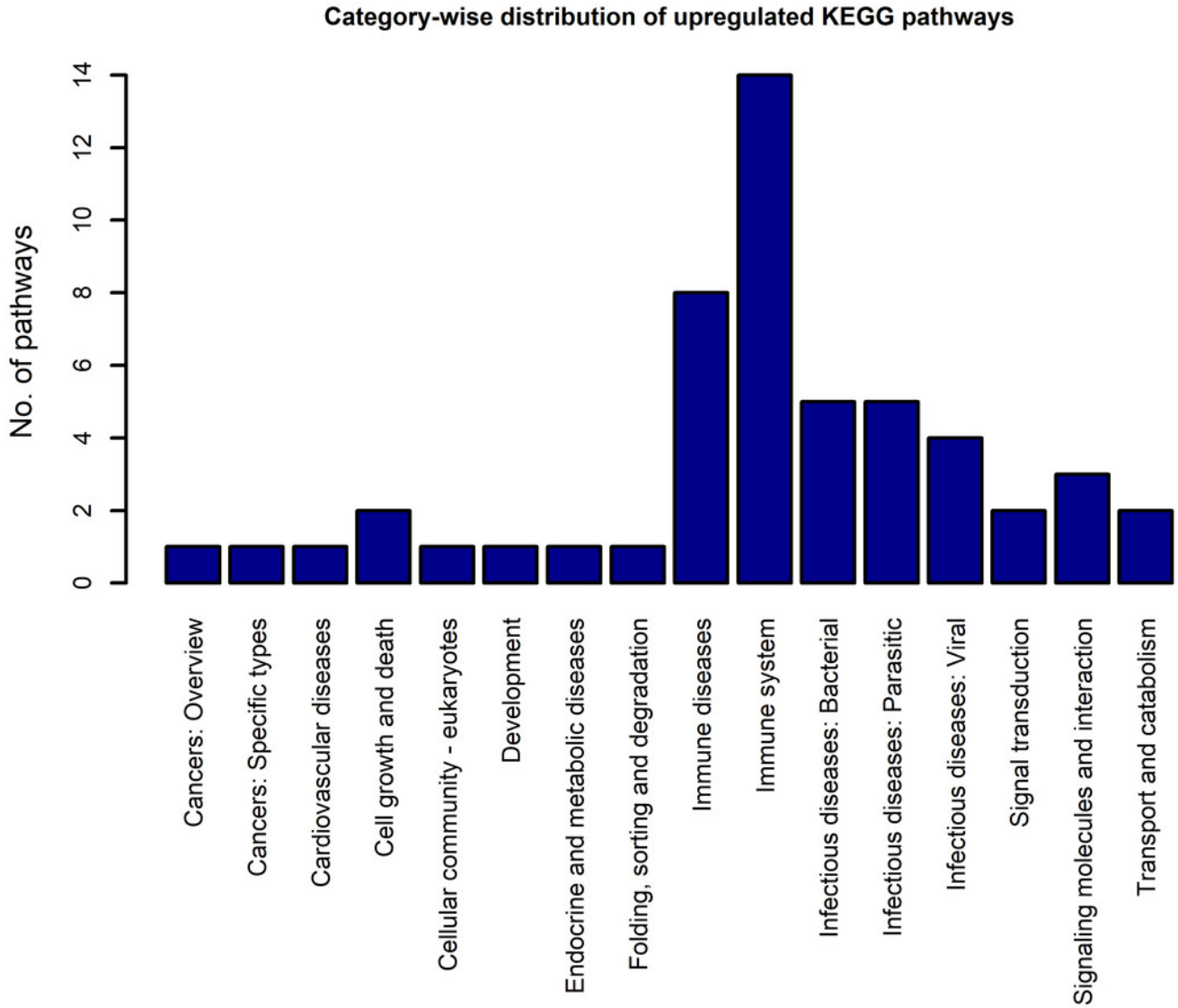

Figure 5

The KEGG category-wise distribution of the enriched pathways in the downregulated genes of the RA synovium.

The x-axis represents the KEGG categories as listed in the KEGG database whereas the y-axis denotes the number of enriched pathways from our study belonging to the KEGG categories.

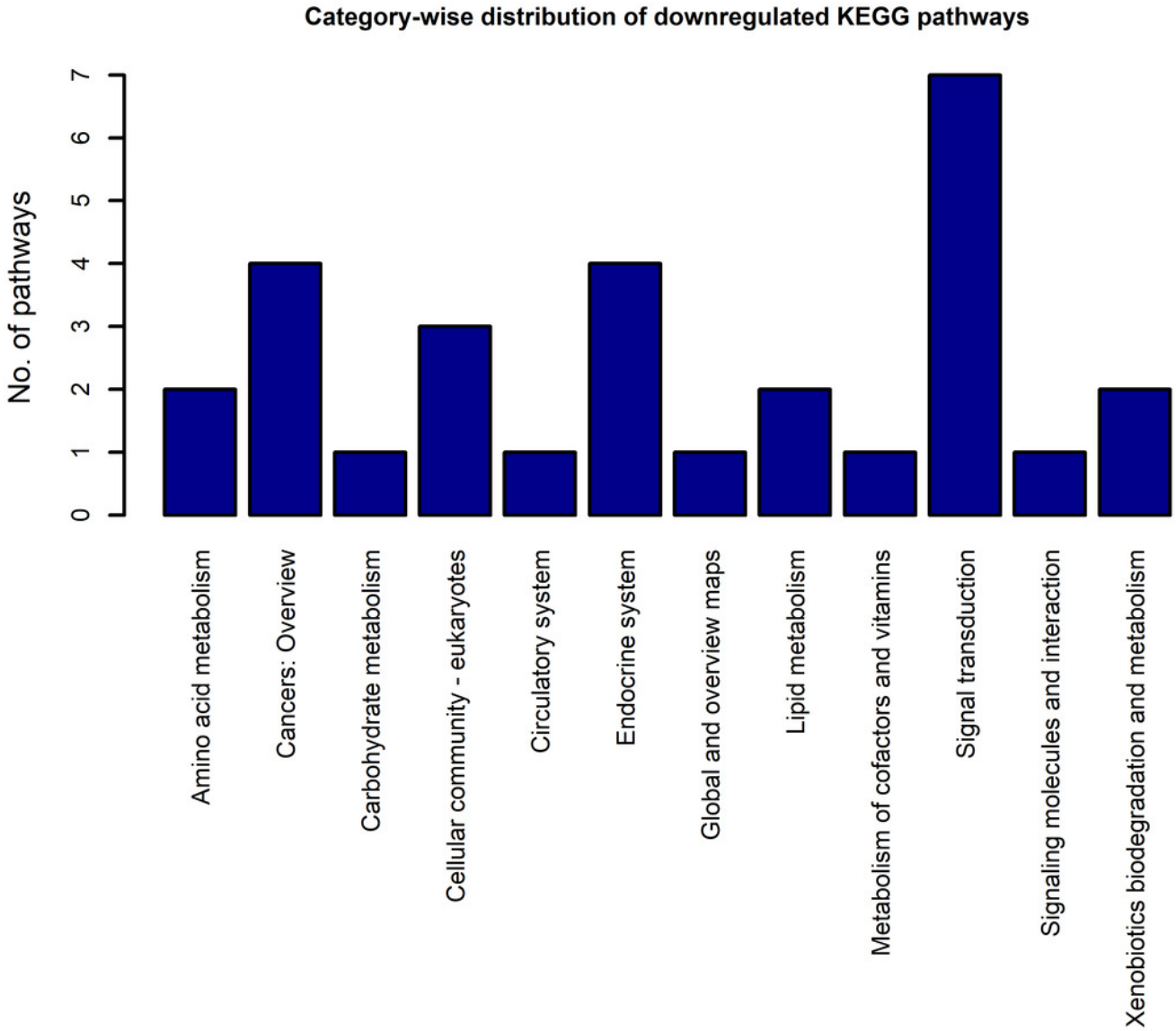

Figure 6

The interaction network of overlapping pathways.

The blue and red pathway nodes denote the process and the signaling pathways respectively. The white pathway nodes denote the other non-disease pathways. The connection between the pathway nodes represents sharing of at least five upregulated or five downregulated genes by the pair of pathway nodes. The size of the node represents the number of genes present in the pathway. Larger nodes show pathways having more number of genes, and smaller nodes represents pathways with lower number of genes.

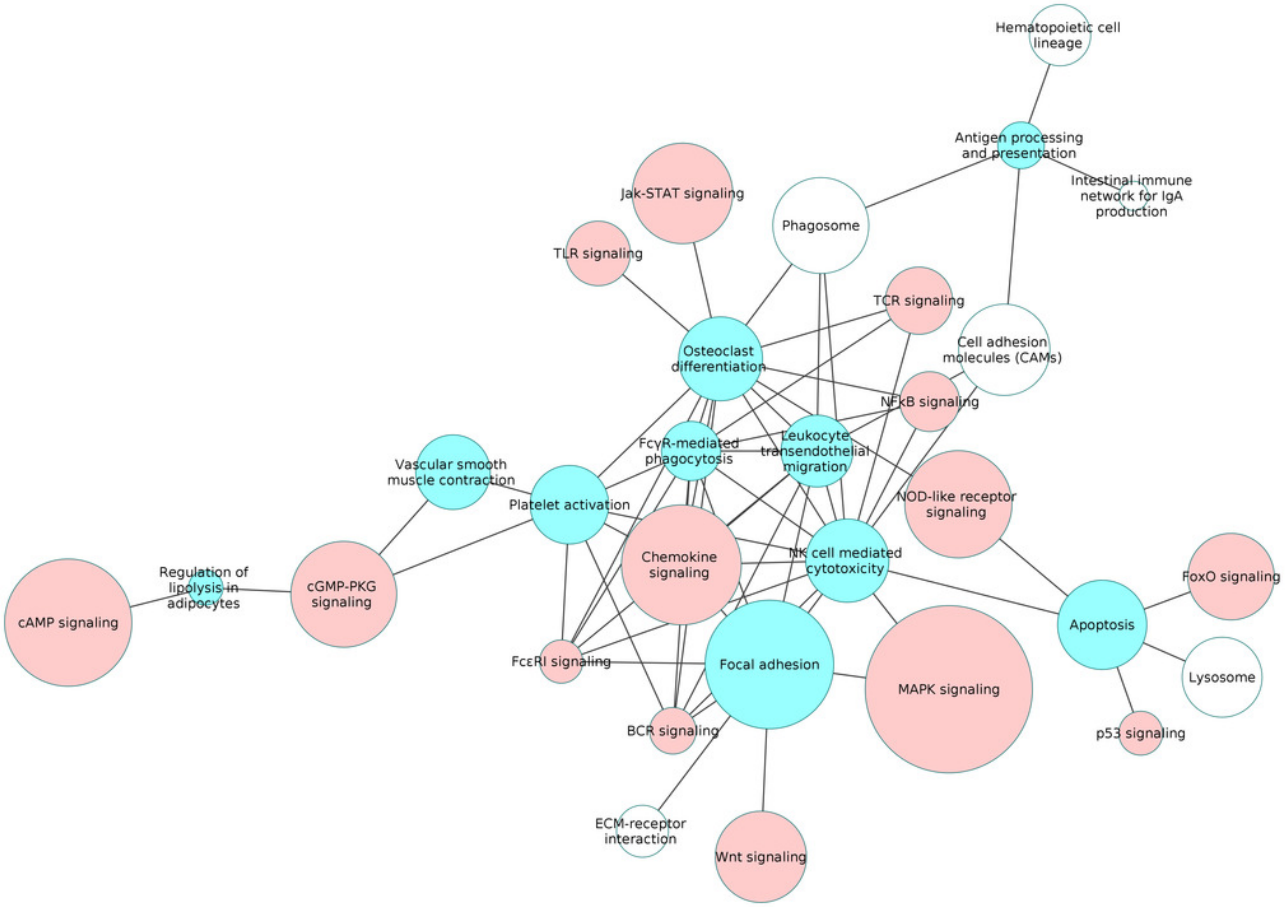

Figure 7

Overlap analysis of the upregulated process pathway osteoclast differentiation with other enriched non-disease pathways in the RA synovium.

The x-axis represents the enriched non-disease pathways with which the osteoclast differentiation pathway share DEGs. The y-axis denotes the number of DEGs shared between the osteoclast differentiation pathway and each of the enriched non-disease pathways. Upregulated signaling pathway genes are shown in light blue and upregulated non-signaling pathway genes in dark blue. The pathway osteoclast differentiation does not share genes with downregulated pathways.

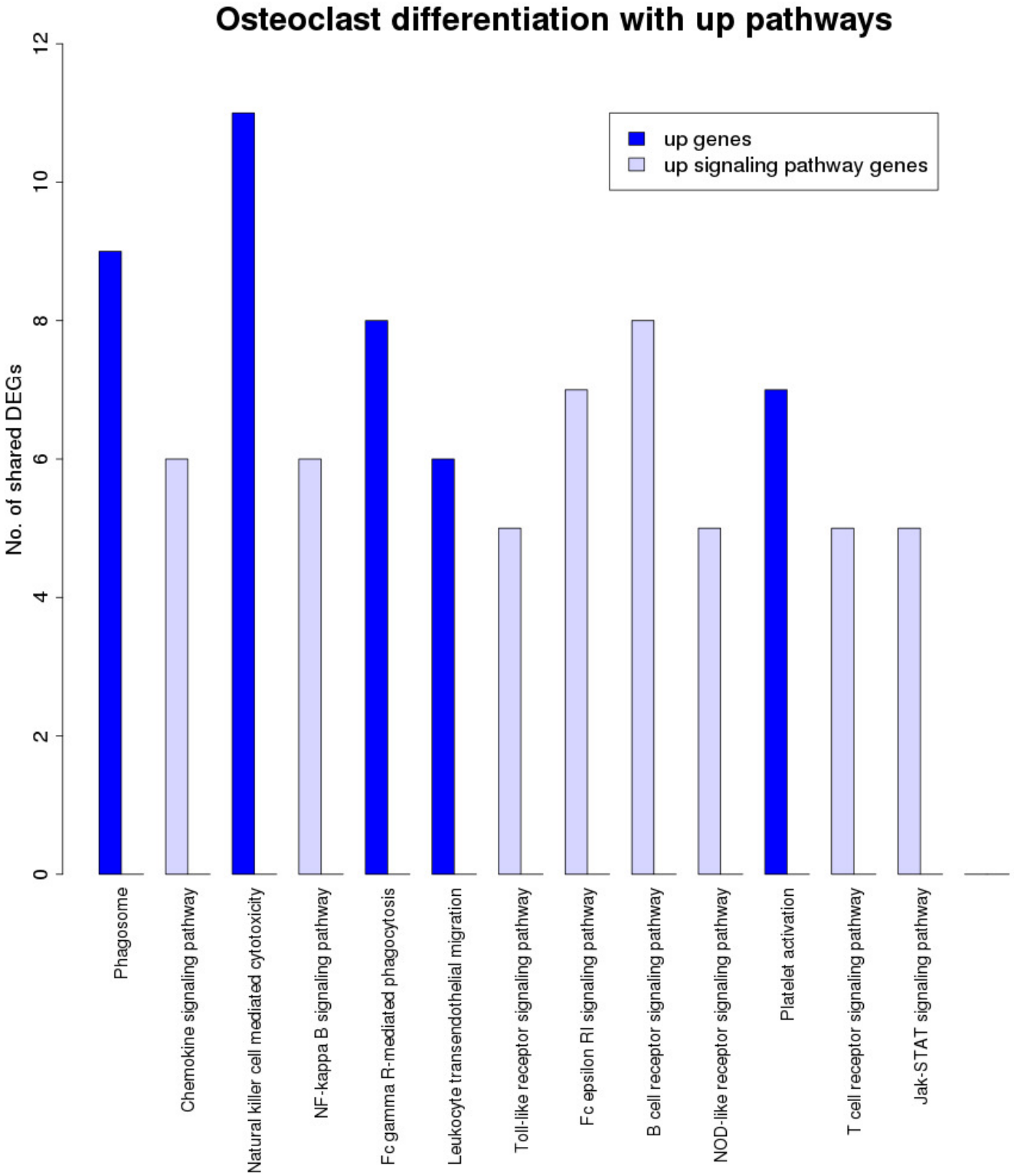
Osteoclast differentiation with up pathways
No. of shared DEGs
0
2
4
6
8
10
12
up genes
up signaling pathway genes
Phagosome
Chemokine signaling pathway
Natural killer cell mediated cytotoxicity
NF-kappa B signaling pathway
Fc gamma R-mediated phagocytosis
Leukocyte transendothelial migration
Toll-like receptor signaling pathway
Fc epsilon RI signaling pathway
B cell receptor signaling pathway
NOD-like receptor signaling pathway
Platelet activation
T cell receptor signaling pathway
Jak-STAT signaling pathway

Figure 8

Overlap analysis of the enriched downregulated process pathways in the RA synovium.

The x-axis represents the enriched non-disease pathways with which the downregulated process pathways share DEGs. The y-axis denotes the number of DEGs shared between the downregulated process pathways and each of the enriched non-disease pathways. Downregulated signaling pathway genes are shown in light pink and downregulated non-signaling pathway genes in red. **(A)** Number of DEGs shared by the pathway “Regulation of lipolysis in adipocytes” with downregulated pathways. **(B)** Number of DEGs shared by the pathway “Vascular smooth muscle contraction” with upregulated pathways. **(C)** Number of DEGs shared by the pathway “Vascular smooth muscle contraction” with downregulated pathways.

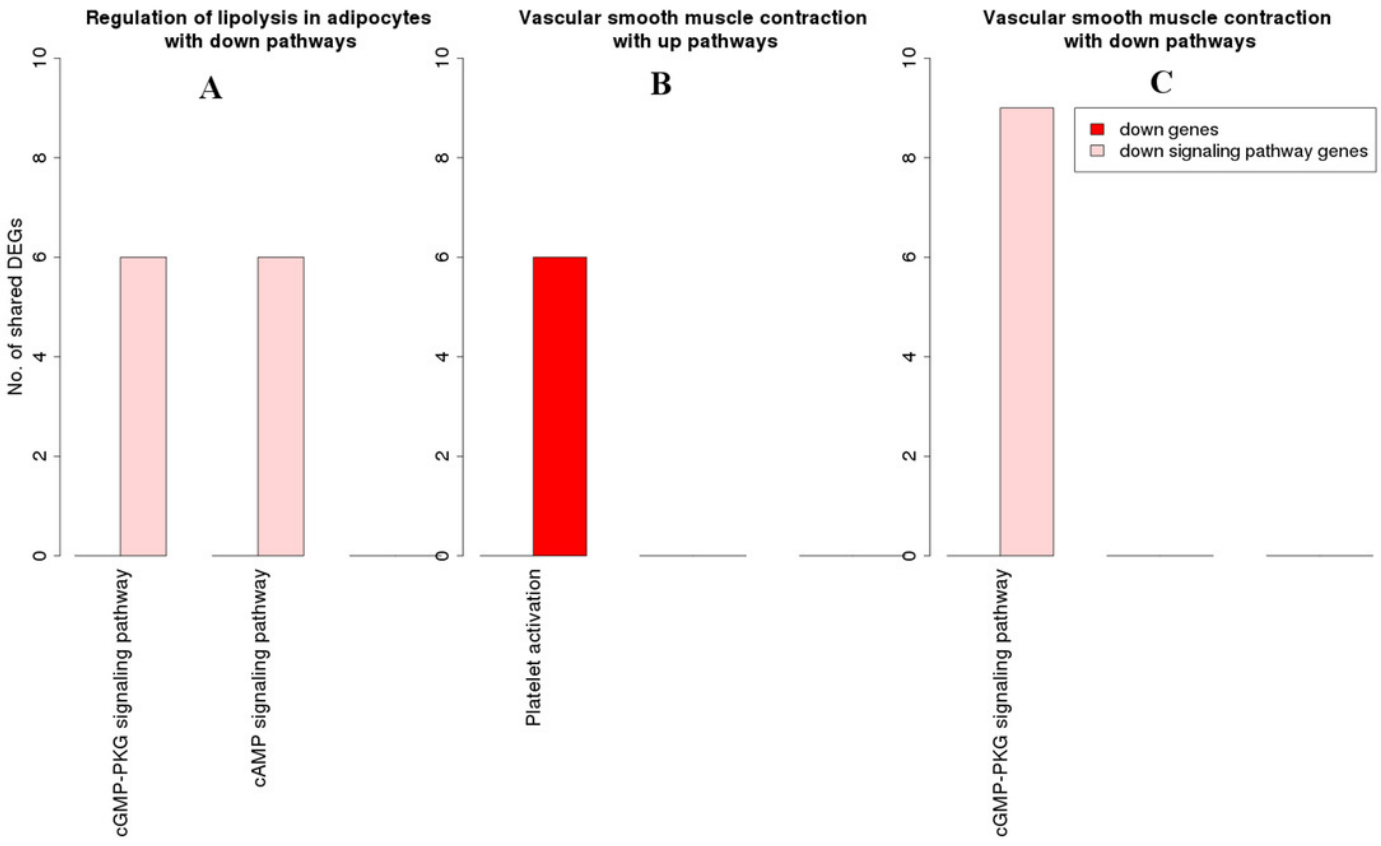

Figure 9

Activation of NF- κB proteins in the osteoclast differentiation network.

The core proteins are represented by thick borders and the shell proteins by thin borders. Rectangle nodes represent the DNA-binding proteins. The RA drug targets are indicated by red borders. The degree of differential regulation of the nodes is denoted as follows: red to grey - downregulation and green – upregulation. The edges of PRKCB are included from literature.

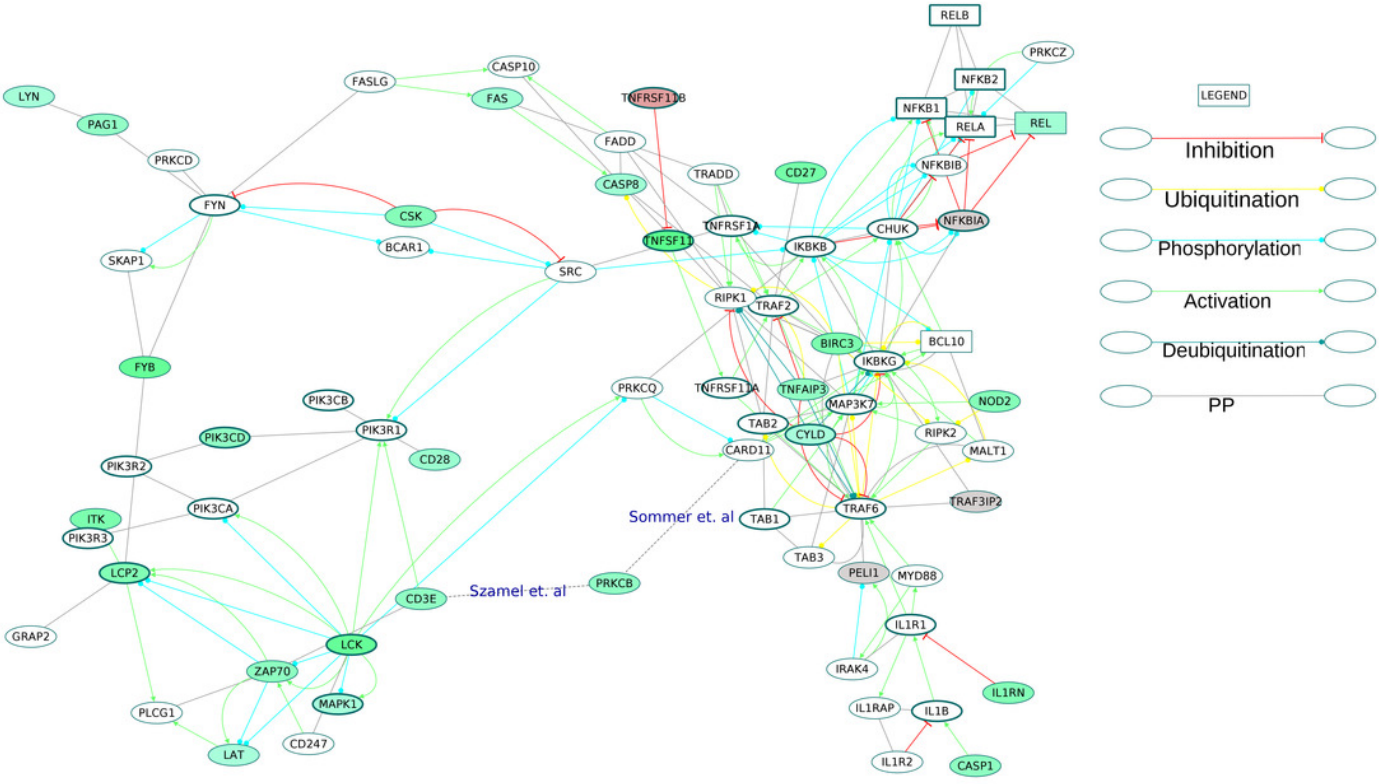

Figure 10

A schematic of enhanced ROS production mediating differentiation of osteoclasts in the RA synovium.

The degree of differential regulation of the nodes in the RA synovium is denoted as follows: red - downregulation and green – upregulation. The cytokine (TNFSF11) and the membrane receptors (CSF1R and CD3E) are above the horizontal line. Genes corresponding to the Nox2 complex and the Forkhead Box proteins are within rectangular boxes. The colors of the edges denote the following: green – activation, red – inhibition, blue – phosphorylation and black – PP. The dotted edges represent the interactions which involve other intermediate molecules. The inhibition of Forkhead box proteins by TNFSF11 are included from literature.